

Complete Theory of Symmetry-based Indicators of Band Topology

Hoi Chun Po,^{1,2} Ashvin Vishwanath,^{1,2,*} and Haruki Watanabe³

¹*Department of Physics, University of California, Berkeley, CA 94720, USA*

²*Department of Physics, Harvard University, Cambridge MA 02138*

³*Department of Applied Physics, University of Tokyo, Tokyo 113-8656, Japan*

The interplay between symmetry and topology leads to a rich variety of electronic topological phases, protecting states such as topological insulators and Dirac semimetals. Here we focus on a different aspect of this interplay, where symmetry unambiguously indicates the presence of a topological band structure. Our study is comprehensive, encompassing all 230 space groups, and is built on two key advances. First, we find an efficient way to represent band structures in terms of elementary basis states, which are readily computed for each space group. Next, we isolate topological band structures by removing the set that represent simple atomic insulators, corresponding to localized Wannier orbitals. Special cases of our theory include the Fu-Kane parity criterion for inversion symmetric \mathbb{Z}_2 topological insulators, and the previously described filling-enforced quantum band insulators. We also describe new results and applications to the search for topological materials.

I. INTRODUCTION

The discovery of topological insulators (TIs) has reinvigorated the well established theory of electronic band structures [1, 2]. Exploration along this new dimension has led to an ever-growing arsenal of topological materials, which include, for instance, topological (crystalline) insulators [3–5], quantum anomalous Hall insulators [6], and Weyl and Dirac semimetals [7]. Such materials possess unprecedented physical properties, like quantized response and gapless surface states, that are robust against all symmetry-preserving perturbations as long as a band picture remains valid [1, 2, 7].

Soon after these new developments, it was realized that symmetries of energy bands, a thoroughly studied aspect of band theory, is also profoundly intertwined with topology. This is exemplified by the celebrated Fu-Kane criterion for inversion-symmetric materials, which demarcates TIs from trivial insulators using only their parity eigenvalues [8]. This criterion, when applicable, greatly simplifies the topological analysis of real materials, and underpins the theoretical prediction and subsequent experimental verification of many TIs [8–12].

It is of fundamental interest to obtain results akin to the Fu-Kane criterion in other symmetry settings. Early generalizations in systems with broken time-reversal (TR) symmetry in 2D constrained the Chern number (C). The eigenvalues of an n -fold rotation was found to determine C modulo n [13–15]. This is characteristic of a symmetry-based indicator of topology—when the indicator is nonvanishing, band topology is guaranteed, but certain topological phases (i.e. C a multiple of n in this context) may be invisible to the indicator. In 3D, it was also recognized that spatial inversion alone can protect nontrivial phases. A new feature here is that these phases do not host protected surface states, since inversion symmetry is broken at the surface, but they do represent distinct phases of matter. For example they possess nontrivial Berry phase structure in the Brillouin Zone which leads to robust entanglement signatures [13, 14, 16, 17] and, in some cases, quan-

tized responses [13, 14, 18]. Interestingly, in the absence of TR invariance the inversion eigenvalues (i.e. parities) can also protect Weyl semimetals [13, 14], which informed early work on materials candidates [19]. Hence this symmetry-based diagnosis is relevant both to the search for nontrivial insulating phases, and also to the study of topological semimetals. It is also important to note that the goal here is distinct from the classification of topological phases, but is instead to identify signatures of band topology in the symmetry transformations of the state.

Can these powerful symmetry indicators for band topology be extended to all space groups (SGs)? Earlier studies have emphasized the topological perspective, which typically rely on constructions that are specifically tailored to a particular topological phase of interest [8, 15]. Such an approach faces an inherent challenge stemming from the sheer multitude of physically relevant symmetry settings—there are 230 SGs in 3D, and each of them is further enriched by the presence or absence of both spin-orbit coupling (SOC) and TR symmetry.

Here we take a complementary, symmetry-focused perspective, which leverages the existing exhaustive results on band symmetries [20, 21] to simplify the analysis. Previous work along these lines has covered restricted cases [13, 14, 22]. For instance, in Ref. [22], which focuses on systems in the 17 2D wallpaper groups without any additional symmetry, such an approach was adopted to help develop a more physical understanding of the mathematical treatment of Ref. [23]. However, the notion of ‘nontrivial’ is a relative concept in these approaches. While such formulation is well-suited for the study of phase transitions between different systems in the same symmetry setting, it does not always indicate the presence of underlying band topology. As an extreme example, such classifications generally regard atomic insulators with different electron fillings as distinct phases, although all the underlying band structures are topologically trivial.

In contrast, our approach will only probe the underlying band topology, and will seek to isolate the relevant symmetry indicators. At the crux of our analysis is the observation that topological band structures arise whenever there is a mismatch between momentum-space and real-space solutions to symmetry constraints [24]. While atomic insulators, which by definition possess localized Wannier orbitals, can be un-

* Corresponding author: avishwanath@g.harvard.edu

derstood from a real-space picture with electrons occupying definite positions as if they were classical particles, topological band structures (that are intrinsic to dimensions greater than one) do not admit such a description. Whenever there is an obstruction to such a real-space reinterpretation, despite the presence of a band gap, the insulating state can only be described through the quantum interference of electrons, and we refer in general to such systems as ‘quantum band insulators’ (QBIs). While all topological phases such as Chern insulators, weak and strong \mathbb{Z}_2 topological insulators and topological crystalline insulators with protected surface states in $d > 1$ are QBIs, more generally, QBIs may or may not have surface states, as the protecting symmetries are not necessarily compatible with any surface termination. Nonetheless, they represent distinct phases of matter, and showcase nontrivial Berry phase in the Brillouin Zone [25], robust entanglement signatures [13, 14, 16, 24], and sometimes quantized responses [13, 14, 18].

Building on this insight, we develop an efficient strategy for identifying topological materials indicated by symmetries. We will first outline a simple framework to organize the set of all possible band structures using only their symmetry labels. By extending the ideas in Refs. [13, 22] and allowing for both addition (stacking) as well as formal subtractions of bands, we show that band structures can be conveniently represented in terms of a special type of Abelian group, which is simply called a ‘lattice’ in mathematical nomenclature. Next, we systematically isolate topological band structures by quotienting out those that can arise from a Wannier description. We perform this computation for all of the 230 SGs, covering all cases with or without TR symmetry and SOC. Our scheme automatically encompasses all previous results concerning symmetry indicators of band topology, including in particular the Fu-Kane criterion, the relation between Chern numbers and rotation eigenvalues, and the inversion-protected nontrivial phases.

We also discover new settings for finding topological materials, including both insulators and semimetals. In particular, we will point out that, in the presence of inversion symmetry, stacking two strong 3D TIs will not simply result in a trivial phase, despite all the \mathbb{Z}_2 indices have been trivialized. Instead, it is shown to produce a QBI, which can be diagnosed through its robust gapless entanglement spectrum. As such band topology is uncovered from the symmetry representations of the bands, we will refer to it as being ‘represented-enforced’. We also discuss a more constrained approach where one first specifies the microscopic lattice degrees of freedom. This is relevant to materials where a hierarchy of energy scales isolates a group of atomic orbitals. We find examples where these constraints lead to semimetallic behavior despite band insulators at the same filling are symmetry-allowed. We will refer to these as ‘lattice-enforced’ semimetals and give a concrete tight-binding example of them. Generalizations of these approaches should aid in the discovery of experimentally relevant topological semimetals and insulators.

Finally, we make two remarks. First, we ignore electron-electron interactions. Second, while our approach is applicable in any dimension, in the special case of 1D even topo-

logical phases are smoothly connected to atomic insulators [26], and therefore are regarded as trivial within our framework. These states, and their descendants in higher dimensions, are collectively known as ‘frozen polarization’ insulators [13], and will be absent from our discussion.

II. BAND STRUCTURES FORM AN ABELIAN GROUP

We will first argue that the possible set of band structures symmetric under an SG \mathcal{G} can be naturally identified as the group $\mathbb{Z}^{d_{\text{BS}}} \equiv \mathbb{Z} \times \mathbb{Z} \times \dots \times \mathbb{Z}$, where d_{BS} is a positive integer that depends on both \mathcal{G} and the spin of the particles (Fig. 1a). We will first set aside TR symmetry, and later discuss how it can be easily incorporated into the same framework. The discussion in this section follows immediately from well established results concerning band symmetries [20], and the same set of results was recently utilized in Ref. [22] to discuss an alternative way to understand the more formal classification in Ref. [23]. Although there is some overlap between the discussion here and that in Ref. [22], we will focus on a different aspect of the narration: Instead of being solely concerned with the values of d_{BS} , we will be more concerned with utilizing this framework to extract other physical information about the systems. As an intermediate step we also perform the first computation of d_{BS} for the 230 space groups (Appendix G).

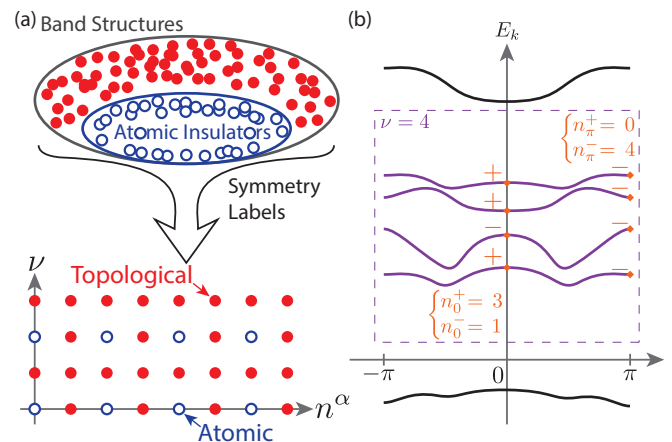


FIG. 1. **Diagnosing band topology using symmetry labels.** (a) Symmetry labels (e.g. ν and n^α) provide a powerful handle to organize the set of band structures obeying the same set of symmetries. Oftentimes they provide an easy way to diagnose whether a band structure is topological or if it can be interpreted as arising from an atomic insulator, which is a trivial state according to our definition. (b) Symmetry labelling of bands in a 1D inversion-symmetric example. Insofar as symmetries are concerned, a target set of bands (boxed) can be labeled by integers corresponding to the multiplicities ($n_{k_0}^\pm$) of the allowed symmetry representations at high-symmetry momenta (diamonds).

We begin by reviewing some basic notions using a simple example. Consider free electrons in a 1D, inversion-symmetric crystal. The energy bands $E_m(k)$ are naturally labeled by the band index m and the crystal momentum $k \in$

$(-\pi, \pi]$. Since inversion P flips $k \leftrightarrow -k$, the Bloch Hamiltonian $H(k)$ is symmetric under $PH(k)P^{-1} = H(-k)$, which implies $E_m(k) = E_m(-k)$, and the wavefunctions are similarly related. The two momenta $k_0 = 0$ and π are special as they satisfy $P(k_0) = k_0$ (up to a reciprocal lattice vector). As such, the symmetry constraint imposed by P becomes a local constraint at k_0 , which implies the wavefunctions $\psi_m(k_0)$ (generically) furnish ‘irreducible representations’ (irreps) of P : $\psi_m^\dagger(k_0)P\psi_m(k_0) = \zeta_m(k_0)$ with $\zeta_m(k_0) = \pm 1$.

The parities $\zeta_m(k_0) = \pm 1$ can be regarded as local (in momentum space) symmetry labels for the energy band $E_m(k)$, and such labels can be readily lifted to a global one assigned to any set of bands separated from others by a band gap. We will refer to such sets of bands as ‘band structures’ (BSs), though, as we will explain, caution has to be taken when this notion is used in higher dimensions. Insofar as symmetries are concerned, we can label the BS by its filling, ν , together with the four non-negative integers, $n_{k_0}^\pm$, corresponding to the multiplicity of the irrep \pm at the momenta $k_0 = 0$ or π (Fig. 1b). Generally, such labels are not independent, since the assumption of a band gap, together with the continuity of the energy bands, cast global symmetry constraints on the symmetry labels. These constraints are known as ‘compatibility relations’. For our 1D problem at hand, there are only two of them, which arise from the filling condition: $\nu = n_0^+ + n_0^- = n_\pi^+ + n_\pi^-$. Consequently the BS is fully specified by three non-negative integers, which we can choose to be n_0^+ , n_π^+ and ν .

This discussion to this point is similar to that of Ref. [22], but we now depart from the combinatorics point of view of that work. Instead, similar to Ref. [13] we develop a mathematical framework to efficiently characterize energy bands in terms of their symmetry transformation properties, and then show that it provides a powerful tool for the analyzing of general band structures. To begin, we first note that any BS in this 1D, inversion-symmetry problem can be represented by a five-component ‘vector’ $\mathbf{n} \equiv (n_0^+, n_0^-, n_\pi^+, n_\pi^-, \nu) \in \mathbb{Z}_{\geq 0}^5$, where $\mathbb{Z}_{\geq 0}$ denotes the set of non-negative integers. In addition, \mathbf{n} is subjected to the two (independent) compatibility relations. We can arrange these relations into a system of linear equations and denote them by a 2×5 matrix \mathcal{C} . The admissible BSs then satisfy $\mathcal{C}\mathbf{n} = \mathbf{0}$, and hence $\ker \mathcal{C}$, the solution space of \mathcal{C} , naturally enters the physical discussion. For the current problem, $\ker \mathcal{C}$ is 3-dimensional, which echoes with the claim that the BS is specified by three non-negative integers. At this point, however, it is natural to make a mathematical abstraction and lift the physical condition of non-negativity, and thereby define

$$\{\text{BS}\} \equiv \ker \mathcal{C} \cap \mathbb{Z}^D, \quad (1)$$

where for the 1D problem at hand we have $D = 5$. The main advantage of this abstraction is that, unlike $\mathbb{Z}_{\geq 0}^D$, \mathbb{Z}^D is an abelian group, which has simple structures that greatly simplify our forthcoming analysis. In particular, $\{\text{BS}\}$ so defined can be identified with $\mathbb{Z}^{d_{\text{BS}}}$, where $d_{\text{BS}} = 3$ is the dimension of the solution space $\ker \mathcal{C}$. Physically, the ‘addition’ in $\mathbb{Z}^{d_{\text{BS}}}$ corresponds to the stacking of energy bands.

Next, we generalize the discussion to any SG \mathcal{G} in three dimensions [27]. We call a momentum $\mathbf{k} \in \text{BZ}$ a ‘high-

symmetry momentum’ if there is any $g \in \mathcal{G}$ other than the lattice translations such that $g(\mathbf{k}) = \mathbf{k}$ (up to a reciprocal lattice vector). We define a ‘band structure’ as a set of energy bands isolated from all others by band gaps above and below at all high-symmetry momenta. Note that in 3D, ‘all high-symmetry momenta’ include all high-symmetry points, lines and planes. The discussion for the 1D example carries through, except that one has to consider a much larger zoo of irreps and compatibility relations (Appendix A). Nonetheless, the main conclusion remains unchanged, and one simply finds

$$\{\text{BS}\} \simeq \mathbb{Z}^{d_{\text{BS}}}, \quad (2)$$

where $d_{\text{BS}} = \dim \ker \mathcal{C}$.

While Eq. (2) follows readily from definitions, it has interesting physical implications. As a group, $\mathbb{Z}^{d_{\text{BS}}}$ is generated by d_{BS} independent generators. In the additive notation, natural for an abelian group, we can write the generators as $\{\mathbf{b}_i : i = 1, \dots, d_{\text{BS}}\}$, and for any given BS we can ‘expand’ it similar to elements in a vector space

$$\text{BS} = \sum_{i=1}^{d_{\text{BS}}} m_i \mathbf{b}_i, \quad (3)$$

where $m_i \in \mathbb{Z}$ are uniquely determined once the basis is fixed. Therefore, full knowledge of $\{\text{BS}\}$ is obtained once the d_{BS} generators \mathbf{b}_i are specified. In particular, the physical BSs, which satisfy the additional non-negative condition, are also elements of $\{\text{BS}\}$, and hence the same expansion applies.

So far, we have not addressed the effect of TR symmetry, which, being anti-unitary, does not lead to new irreps when it is incorporated [20]. Instead, TR symmetry will generally force certain irreps to become paired with either itself or another (Appendix C). When an irrep α at \mathbf{k} is paired with a different irrep β under TR, we simply add to \mathcal{C} an additional compatibility relation $n_{\mathbf{k}}^\alpha = n_{\mathbf{k}}^\beta$; when α is paired with itself, we demand α to be an even integer, which can be achieved by redefining $\tilde{n}_{\mathbf{k}}^\alpha \equiv n_{\mathbf{k}}^\alpha/2$ and a corresponding rewriting of \mathcal{C} in terms of $\tilde{\mathbf{n}}$. In brief, all TR constraints can be incorporated in a simple manner in the described framework, and therefore we will treat them on equal footings with SG constraints from now on.

III. ATOMIC INSULATORS AND MISMATCH CLASSIFICATION

While we have provided a systematic framework to probe the structure of $\{\text{BS}\}$, much insight can be gleaned from a study of atomic insulators (AIs). AIs correspond to band insulators constructed by first specifying a symmetric set of lattice points in real space, and then fully occupying a set of local orbitals on each of the lattice sites. The possible set of AIs can be easily read off from tabulated data of SGs [21, 28]. In addition, once the real-space degrees of freedom are specified one can readily compute the corresponding element in $\{\text{BS}\}$ (Appendix B). As stacking two AIs lead to a new AI, we see that $\{\text{AI}\} \leq \{\text{BS}\}$ as groups. Any subgroup of $\mathbb{Z}^{d_{\text{BS}}}$ is again

a free, finitely-generated abelian group, and therefore we conclude

$$\{\text{AI}\} \simeq \mathbb{Z}^{d_{\text{AI}}} \equiv \left\{ \sum_{i=1}^{d_{\text{AI}}} m_i \mathbf{a}_i : m_i \in \mathbb{Z} \right\}, \quad (4)$$

where we denote by $\{\mathbf{a}_i\}$ a complete set of basis for $\{\text{AI}\}$.

Once $\{\text{BS}\}$ and $\{\text{AI}\}$ are separately computed, it is straightforward to evaluate the quotient group (Appendix D)

$$X_{\text{BS}} \equiv \frac{\{\text{BS}\}}{\{\text{AI}\}}. \quad (5)$$

Physically, an entry in X_{BS} corresponds to an infinite class of BSs that, while distinct as elements of $\{\text{BS}\}$, only differ from each other by the stacking of an AI. By definition, the entire subgroup $\{\text{AI}\}$ collapses into the trivial element of X_{BS} . Conversely, any nontrivial element of X_{BS} corresponds to BSs that cannot be interpreted as AIs, and therefore X_{BS} serves as a symmetry indicator of topological BSs.

Following the described recipe, we compute X_{BS} for all 230 SGs in the four symmetry settings mentioned. The results for spinful fermions with TR symmetry, relevant for real materials with significant SOC and no magnetic order, are tabulated in Table I. The other results are presented in Appendix G. An interesting observation from this exhaustive computation is the following: for all the symmetry settings considered, we found $d_{\text{BS}} = d_{\text{AI}}$, and therefore X_{BS} is always a finite abelian group. Equivalently, when only symmetry labels are used in the diagnosis, a BS is nontrivial iff it can only be understood as a ‘fraction’ of an AI. In addition, the finiteness of X_{BS} implies that a complete set of basis for $\{\text{BS}\}$ can be found by studying combinations of AIs, similar to Eq. (4) but with a generalization of the expansion coefficients $m_i \in \mathbb{Z}$ to $q_i \in \mathbb{Q}$, subjected to the constraint that the sum remains integer-valued. Therefore, the basis of $\{\text{BS}\}$ can be readily computed by combining existing SG data [20, 21] with our discussion on AI in Appendix B.

To illustrate the ideas more concretely, we discuss a simple example concerning spinless fermions without TR invariance, but symmetric under SG **106**. In this setting, $d_{\text{BS}} = d_{\text{AI}} = 3$, and \mathbf{a}_1 , one of the three generators of $\{\text{AI}\}$, has the property that all irreps appear an even number of times, while the other two generators contain some odd entries. Now consider $\mathbf{b}_1 \equiv \mathbf{a}_1/2$, which is still integer-valued. Clearly, the linearity of the the problem implies \mathbf{b}_1 satisfies all symmetry constraints, and therefore $\mathbf{b}_1 \in \{\text{BS}\}$. However, $\mathbf{b}_1 \notin \{\text{AI}\} \equiv \{\sum_{i=1}^3 m_i \mathbf{a}_i : m_i \in \mathbb{Z}\}$, and therefore \mathbf{b}_1 corresponds to a quantum BS, and indeed it is a representative for the nontrivial element of $X_{\text{BS}} = \mathbb{Z}_2$. In addition, if we consider a tight-binding model with representation content corresponding to \mathbf{a}_1 , the decomposition $\mathbf{a}_1 = \mathbf{b}_1 + \mathbf{b}_1$ implies it is possible to open a band gap at all high-symmetry momenta at half filling, and thereby realizing the quantum BS \mathbf{b}_1 . It turns out that, in fact, \mathbf{b}_1 corresponds to a ‘filling-enforced’ QBI (feQBI) [24].

TABLE I. Symmetry indicator of topological band structures, X_{BS} , for time-reversal symmetric systems with significant spin-orbit coupling. Space groups (SGs) with a trivial $X_{\text{BS}} = \mathbb{Z}_1$ are omitted. The SG numbers are color-coded based on whether the adjectives {Centrosymmetric, Symmorphic} apply (‘+’) or not (‘-’): black = {+,+}, green = {+,-}, purple = {-,+}, and red = {-,-}. Note that, thanks to the the Fu-Kane criterion, all centrosymmetric SGs have nontrivial X_{BS} .

| X_{BS} | SGs |
|--|---|
| \mathbb{Z}_2 | <i>81, 82, 111, 112, 113, 114, 115, 116, 117</i> <i>118, 119, 120, 121, 122, 215, 216, 217, 218</i> <i>219, 220</i> |
| \mathbb{Z}_3 | <i>188, 190</i> |
| \mathbb{Z}_4 | <i>52, 56, 58, 60, 61, 62, 70, 88, 126</i> <i>130, 133, 135, 136, 137, 138, 141, 142, 163</i> <i>165, 167, 202, 203, 205, 222, 223, 227, 228</i> <i>230</i> |
| \mathbb{Z}_8 | <i>128, 225, 226</i> |
| \mathbb{Z}_{12} | <i>176, 192, 193, 194</i> |
| $\mathbb{Z}_2 \times \mathbb{Z}_4$ | <i>14, 15, 48, 50, 53, 54, 55, 57, 59</i> <i>63, 64, 66, 68, 71, 72, 73, 74, 84</i> <i>85, 86, 125, 129, 131, 132, 134, 147, 148</i> <i>162, 164, 166, 200, 201, 204, 206, 224</i> |
| $\mathbb{Z}_2 \times \mathbb{Z}_8$ | <i>87, 124, 139, 140, 229</i> |
| $\mathbb{Z}_3 \times \mathbb{Z}_3$ | <i>174, 187, 189</i> |
| $\mathbb{Z}_4 \times \mathbb{Z}_8$ | <i>127, 221</i> |
| $\mathbb{Z}_6 \times \mathbb{Z}_{12}$ | <i>175, 191</i> |
| $\mathbb{Z}_2 \times \mathbb{Z}_2 \times \mathbb{Z}_4$ | <i>11, 12, 13, 49, 51, 65, 67, 69</i> |
| $\mathbb{Z}_2 \times \mathbb{Z}_4 \times \mathbb{Z}_8$ | <i>83, 123</i> |
| $\mathbb{Z}_2 \times \mathbb{Z}_2 \times \mathbb{Z}_2 \times \mathbb{Z}_4$ | <i>2, 10, 47</i> |

We will elaborate further on this point in the subsequent sections.

Before we move on to concrete applications of our results, we pause to clarify some subtleties in the exposition. Recall that the notion of BS is defined using the presence of band gaps at all high-symmetry momenta. Generally, however, there can be gaplessness in the interior of the BZ that coexist with our definition of BS. While in some cases such gaplessness is accidental in nature, in the sense that it can be annihilated without affecting the BS, in some more interesting cases it is enforced by the specification of the symmetry content. This was pointed out in Refs. [13, 14] for inversion-symmetric systems without TR symmetry, where certain assignment of the parity eigenvalues ensures the presence of Weyl points at some generic momenta. When a nontrivial element in X_{BS} can be insulating, we refer to it as a ‘representation-enforced QBI’ (reQBI); when it is necessarily gapless, we call it a ‘representation-enforced semimetals’ (reSM). We caution that X_{BS} will naturally include *both* reQBIs and reSMs, although some symmetry settings naturally forbid the notion of reSMs. In fact, one can show that their individual diagnoses are related by $X_{\text{SM}} = X_{\text{BS}}/X_{\text{BI}}$ (Appendix E 1). Hence, given an entry of X_{BS} one has to further

decide whether it corresponds to a reSM or a reQBI. We will provide an explicit example of such arguments in Appendix E 3, but a more general discussion on this further diagnosis will be left for future work.

In addition, we also note that while *every* BS in X_{BS} is necessarily nontrivial, some systems in the trivial class can also be topological. Such is the case whenever the topological nature of the band structure is undetectable using only symmetry labels, say for the tenfold way phases in the absence of any spatial symmetries. Some of the feQBIs we discussed in Ref. [24] also fall into this category, since their non-atomic nature is only exposed upon enforcing extra physical conditions in the analysis (Appendix F 3), which is not captured within the group structure of $\{\text{BS}\}$ and $\{\text{AI}\}$.

IV. APPLICATIONS

A. New quantum band insulators in conventional settings

As a first application, we utilize the results in Table I to look for reQBIs that are not diagnosed by previously available topological invariants. In particular, we will focus on an interesting result concerning one of the most well studied symmetry setting: materials with significant SOC symmetric under TR, lattice translations and inversion (SG 2).

As shown in Table I, $X_{\text{BS}} = \mathbb{Z}_2^3 \times \mathbb{Z}_4$ for this setting. Using the Fu-Kane criterion [8], one can readily verify the strong and weak TIs respectively serve as the generators of the \mathbb{Z}_4 and \mathbb{Z}_2 factors. This identification, however, fails to account for the nontrivial nature of the ‘doubled’ strong TI, which being a nontrivial element in \mathbb{Z}_4 corresponds to a reQBI. This reQBI has no protected surface states and a trivial magnetoelectric response ($\theta = 0$), and it cannot be directly explained using earlier works focusing on inversion-symmetric insulators [13, 14, 16].

Nonetheless, similar to the argument in Refs. [13, 14, 16], the nontrivial nature of the reQBI can be seen from its entanglement spectrum, which exhibits protected gaplessness related to the parity eigenvalues of the filled bands (Fig. 2a). In the present context, we define the entanglement spectrum as the collection of single-particle entanglement energies arising from a spatial cut, which contains an inversion center and is perpendicular to a crystalline axis. Yet, one must use caution in interpreting the nontrivial nature of such entanglement, since inversion-symmetric AIs often have protected entanglement surface states. They arise whenever the center of mass of the electronic wavefunction is pinned to the entanglement cut, and such states were called ‘frozen-polarization states’. The presence of such entanglement surface modes is dependent on the arbitrary choice of the location of the cut, and therefore are not as robust as the other topological characterizations. In contrast, since we have already quotient out all AIs in the definition of X_{BS} , the reQBI at hand must have a more topological origin. This is verified from the pictorial argument in Fig. 2a, where we show that the entanglement gaplessness cannot be reconciled with that arising from any AI. Note that if TR is broken, Kramers paring will be lifted and the irrep content

of this reQBI becomes achievable with an AI. This suggests that the reQBI at hand is protected by the combination of TR and inversion symmetry, and in particular it can be interpreted as a TR-symmetric BS mimicking a TR-broken AI through momentum space quantum inference. It is an interesting open question to study whether or not this reQBI has any associated quantized physical response [13].

Since the strong TI is compatible with any additional spatial symmetry, the argument above is applicable to any centrosymmetric SGs. Indeed, as can be seen from Table I, all of them have $|X_{\text{BS}}| \geq 4$, consistent with our claim. From the same table, we can also observe that, very often, a general weak TI becomes incompatible with a higher degree of spatial symmetries [29]. While this has been pointed out for certain cases in the literature [30], our approach automatically encapsulates some of these result in a simple manner. Finally, we remark that while the same X_{BS} is found for SG 2 in all the other symmetry settings (Appendix G), their physical interpretations are very different. In particular, the generators of $\mathbb{Z}_4 < X_{\text{BS}}$ corresponds to a reSM in the other settings.

B. Lattice-enforced semimetals

As another application of our results, consider the following question: Given a specification of the microscopic degrees of freedom (DOF), what are the possible phases of the system? As we demonstrate below, the structure of $\{\text{BS}\}$ will cast strong constraints on the answer. We will in particular focus on the study of semimetals, but a similar analysis can be performed in the study of, say, reQBIs.

As a warm-up, recall the physics of (spinless) graphene, where specifying the honeycomb lattice dictates that the irrep at the K point is necessarily two-dimensional, and therefore the system is guaranteed to be gapless at half filling. Using the structure of $\{\text{BS}\}$ we described, this line of reasoning can be efficiently generalized to an arbitrary symmetry setting: Any specification of the lattice DOF corresponds to an element $\mathbf{A} \in \{\text{AI}\}$, and one simply asks if it is possible to write $\mathbf{A} = \mathbf{B}_\nu + \mathbf{B}_c$, where $\mathbf{B}_{\nu,c} \in \{\text{BS}\}$ satisfies the physical non-negative condition, such that \mathbf{B}_ν corresponds to a BS with a specified filling ν . Whenever the answer is no, the system is guaranteed to be (semi-)metallic. We refer to any such system as a ‘lattice-enforced semimetal’ (leSM). Note that a stronger form of symmetry-enforced gaplessness can originate simply from the electron filling, and such systems were dubbed as ‘filling-enforced semimetal’ (feSMs) [31, 32]. We will exclude feSMs from the definition of leSMs, i.e. we only call a system a leSM if the filling ν is compatible with some band insulators in the same symmetry setting, but is nonetheless gapless because of the additional lattice constraints.

A preliminary analysis reveals that leSMs abound, especially for spinless systems with TR symmetry. This is in fact anticipated from the earlier discussions in Refs. [33–35]. Instead, we will turn our attention to TR-invariant systems with significant SOC, which lies beyond the scope of these earlier studies and oftentimes leads to interesting new physics [1, 7, 24]. While a systematic survey of them will be the fo-

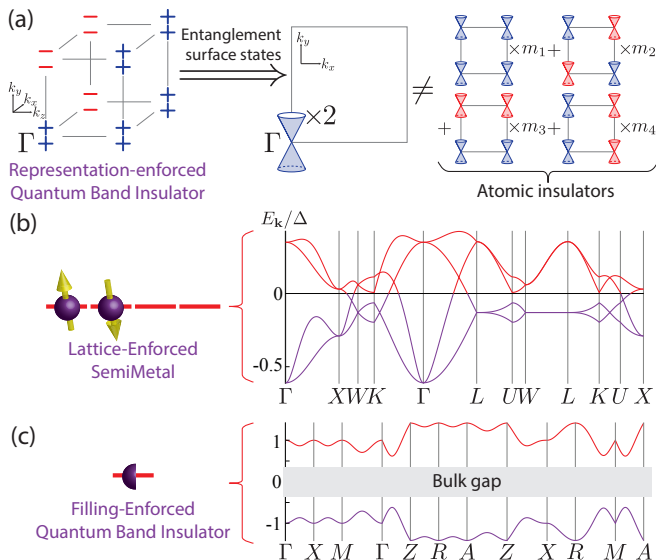


FIG. 2. **New topological band structures** (a) A new representation-enforced quantum band insulator of spinful electrons with time-reversal and inversion symmetries. The strong and weak \mathbb{Z}_2 indices can be computed from the parities of the occupied bands, which we indicate by \pm at the eight time-reversal invariant momenta [8]. The parity from one state of each Kramers pair is shown, and therefore the depicted system has four filled bands. Although all the conventional \mathbb{Z}_2 indices are trivial, the entanglement spectrum at a spatial cut parallel to the x - y plane containing an inversion center features two Dirac cones (blue) at Γ [13, 14, 16]. Such entanglement surface states cannot be reconciled with those arising from atomic insulators, which must arise as integer combination (i.e. $m_i \in \mathbb{Z}$) of definite distribution of the parity-even and odd (blue and red) Dirac cones. (b,c) Local description in terms of filling of orbitals with definite transformation properties (left) can lead to nontrivial consequences in the resulting band structures (right). This can be efficiently analyzed using our results. (b) A partially filled local orbital leads to a band structure with irremovable connectivity, and therefore gives rise to a ‘lattice-enforced semimetal’ with robust semimetallic behavior. (c) In another symmetry setting, a ‘filling-enforced quantum band insulator’ is possible even when the site-filling is fractional for *any* symmetric lattice.

cus of another study, here we present a proof-of-concept leSM example we found. We will only sketch the key features of the model, and the interested readers are referred to Appendix F 1 for details of the analysis.

Consider a TR symmetric, face-centered cubic system with two symmetry-related sites per unit cell, where each site has a local environment corresponding to the cubic point group T . On each site, we let the physical DOF be the p orbitals $p_{x,y,z}$, which in the absence of SOC forms a 3D irrep of T . Incorporating an on-site SOC term $\sim \Delta \mathbf{L} \cdot \mathbf{S}$, where \mathbf{L} and \mathbf{S} respectively denote the orbital and spin angular momentum operators, the degeneracy is lifted by the crystal field according to their spin quantum numbers: $1 \otimes \frac{1}{2} = \frac{1}{2} \oplus \frac{3}{2}$. We suppose the system has a filling of 4 electrons per site and that $\Delta > 0$ is the dominant energy scale, which means that the spin-1/2 doublet is fully filled, and the physically relevant DOF are re-

duced to the half-filled spin-3/2 multiplet from each site. Note that the effective filling is now 2 electrons per site, giving 4 electrons per unit cell.

Although the local orbitals are partially filled, generically a band gap becomes permissible once electron hopping is incorporated. Naively, for the present problem this may appear to be the likely scenario, since the momentum-space irreps all have dimensions ≤ 4 and band insulators are known to be possible at this filling [31, 32]. However, using our framework one can prove that no BS is possible for this system at $\nu = 4$, which implies there will be irremovable lattice-enforced gaplessness at some high-symmetry momentum. This is indeed verified in Fig. 2b, where we plot the band structure obtained from an example tight-binding model (Appendix F 1).

C. Topological band structures in uncharted settings

Finally, we utilize our results to look for new QBIs in previously unexplored symmetry settings. In fact, from our exhaustive computation we can claim discovery of new topological phases whenever we find any uncharted setting with $X_{BS} \neq \mathbb{Z}_1$, the trivial group. Instead of surveying all the new phases we discovered, which we again leave to future works, here we will turn our focus to the study of feQBIs—quantum band insulators diagnosable solely from their filling.

As all possible TR-symmetric feQBIs have been discussed in Ref. [24], we will consider systems without TR invariance. Two key quantities of interest here are the set of possible electron fillings among elements of $\{BS\}$ and $\{AI\}$. Whenever there is a mismatch between the two, it indicates that certain nontrivial element of X_{BS} can be diagnosed simply using the electron filling. This question can again be tackled efficiently using the vector-space like structure of $\{BS\}$ and $\{AI\}$. We found the two sets of fillings always agree for the spinful problem, but a mismatch is found for the following eight SGs for spinless fermions without TR symmetry: **73, 106, 110, 133, 142, 206, 228 and 230**. Note that more mismatch is exposed when one further imposes the physical conditions, which we discuss in more details in Appendix F 2. [36]

As we have cautioned, however, a nontrivial BS can generally be either a reSM or a reQBI. To establish that the filling mismatch described above indeed leads to feQBIs, one has to further assert that a band gap is possible at all *generic* momenta in the BZ. This is achieved in Appendix F 2, where we provide explicit tight-binding models for all the new feQBIs we discovered. An example band structure is plotted in Fig. 2c, which demonstrates that even at a filling of half an electron per site, a band gap is nonetheless possible. Note that these new feQBI examples are, in a sense, more intriguing than the ones we discussed in Ref. [24]. In our previous examples assuming TR-symmetric spinful electrons, the filling condition was enriched by Kramers degeneracy, and feQBIs were discovered at odd-integer site fillings. In these new examples we discovered, however, the site filling is fractional for *any* choice of SG-symmetric lattices. Superficially, this might appear to be at odds with the conventional wisdom that gapped phases at fractional fillings are associated with either discrete

symmetry breaking or intrinsic topological order—both only possible in the presence of interactions. Rather, these examples highlight the fact that spatial symmetries can lead to intriguing constraints between filling and phases, as was discussed in Ref. [31], which, in fact, correctly predicted that symmetry-protected topological phases might be possible for these systems at such fractional fillings (Appendix F 2).

V. DISCUSSION

In this work, we present a simple mathematical framework for efficiently analyzing band structures as entities defined globally over the Brillouin zone. We further utilize this result to systematically quantify the mismatch between the momentum- and real-space descriptions of free electron phases, discovering a plethora of symmetry settings for which new topological materials are possible.

Our results concern a fundamental aspect of the ubiquitous band theory. For electronic problems, we demonstrated the power of our approach by discussing three particular applications, predicting new quantum band insulators and semimet-

als in both conventional and uncharted symmetry settings. Some interesting future directions include: (i) Incorporating the ‘tenfold way’ classification into our symmetry-based diagnosis of topological materials [22]; (ii) Discovering quantized physical responses unique to the new phases we predicted [13, 14, 18]; (iii) Extending the results to magnetic SGs by including the extra compatibility relations [20]; and (iv) Screening of materials database for topological materials relying on fast diagnosis invoking only symmetry labels [37]. More broadly, we expect our analysis to shed light on any other fields of studies, most notably photonics and phononics, where the interplay between topology, symmetry and band structures is of interest.

ACKNOWLEDGMENTS

We thank A. Turner and M. Zaletel for insightful discussions and collaborations on earlier works. AV and HCP were supported by NSF DMR-141134. AV acknowledges support from a Simons Investigator Award.

-
- [1] M. Franz and L. Molenkamp, eds., *Topological Insulators*, Contemporary Concepts of Condensed Matter Science, Vol. 6 (Elsevier, 2013).
 - [2] B. A. Bernevig and T. L. Hughes, *Topological insulators and topological superconductors* (Princeton University Press, 2013).
 - [3] M. Z. Hasan and C. L. Kane, *Rev. Mod. Phys.* **82**, 3045 (2010).
 - [4] L. Fu, *Phys. Rev. Lett.* **106**, 106802 (2011).
 - [5] T. H. Hsieh, H. Lin, J. Liu, W. Duan, A. Bansil, and L. Fu, *Nat. Commun.* **3**, 982 (2012).
 - [6] C.-Z. Chang, J. Zhang, X. Feng, J. Shen, Z. Zhang, M. Guo, K. Li, Y. Ou, P. Wei, L.-L. Wang, Z.-Q. Ji, Y. Feng, S. Ji, X. Chen, J. Jia, X. Dai, Z. Fang, S.-C. Zhang, K. He, Y. Wang, L. Lu, X.-C. Ma, and Q.-K. Xue, *Science* **340**, 167 (2013).
 - [7] A. Bansil, H. Lin, and T. Das, *Rev. Mod. Phys.* **88**, 021004 (2016).
 - [8] L. Fu and C. L. Kane, *Phys. Rev. B* **76**, 045302 (2007).
 - [9] B. A. Bernevig, T. L. Hughes, and S.-C. Zhang, *Science* **314**, 1757 (2006).
 - [10] M. König, S. Wiedmann, C. Brüne, A. Roth, H. Buhmann, L. W. Molenkamp, X.-L. Qi, and S.-C. Zhang, *Science* **318**, 766 (2007).
 - [11] D. Hsieh, D. Qian, L. Wray, Y. Xia, Y. S. Hor, R. Cava, and M. Z. Hasan, *Nature* **452**, 970 (2008).
 - [12] H. Zhang, C.-X. Liu, X.-L. Qi, X. Dai, Z. Fang, and S.-C. Zhang, *Nat. Phys.* **5**, 438 (2009).
 - [13] A. M. Turner, Y. Zhang, R. S. K. Mong, and A. Vishwanath, *Phys. Rev. B* **85**, 165120 (2012).
 - [14] T. L. Hughes, E. Prodan, and B. A. Bernevig, *Phys. Rev. B* **83**, 245132 (2011).
 - [15] C. Fang, M. J. Gilbert, and B. A. Bernevig, *Phys. Rev. B* **86**, 115112 (2012).
 - [16] A. M. Turner, Y. Zhang, and A. Vishwanath, *Phys. Rev. B* **82**, 241102 (2010).
 - [17] M. Taherinejad, K. F. Garrity, and D. Vanderbilt, *Phys. Rev. B* **89**, 115102 (2014).
 - [18] Y.-M. Lu and D.-H. Lee, ArXiv e-prints (2014), [arXiv:1403.5558](https://arxiv.org/abs/1403.5558).
 - [19] X. Wan, A. M. Turner, A. Vishwanath, and S. Y. Savrasov, *Phys. Rev. B* **83**, 205101 (2011).
 - [20] C. J. Bradley and A. P. Cracknell, *The Mathematical Theory of Symmetry in Solids: Representation Theory for Point Groups and Space Groups* (Oxford University Press, 1972).
 - [21] M. I. Aroyo, A. Kirov, C. Capillas, J. M. Perez-Mato, and H. Wondratschek, *Acta Crystallogr. Sect. A* **62**, 115 (2006).
 - [22] J. Kruthoff, J. de Boer, J. van Wezel, C. L. Kane, and R.-J. Slager, ArXiv e-prints (2016), [arXiv:1612.02007](https://arxiv.org/abs/1612.02007).
 - [23] D. S. Freed and G. W. Moore, *Annales Henri Poincaré* **14**, 1927 (2013).
 - [24] H. C. Po, H. Watanabe, M. P. Zaletel, and A. Vishwanath, *Sci. Adv.* **2**, e1501782 (2016).
 - [25] A. Alexandradinata and B. A. Bernevig, *Phys. Rev. B* **93**, 205104 (2016).
 - [26] N. Read, ArXiv e-prints (2016), [arXiv:1608.04696](https://arxiv.org/abs/1608.04696).
 - [27] The general framework applies directly to any spatial dimensions; here we focus on three dimensions for physical reasons.
 - [28] T. Hahn, ed., *International Tables for Crystallography*, 5th ed., Vol. A: Space-group symmetry (Springer, 2006).
 - [29] This is related to the number of factors in X_{BS} , i.e. the number of independent generators N_t . For any centrosymmetric SG, the Fu-Kane criterion dictates that all strong and weak TIs are diagnosable using symmetry labels. As one such factor is reserved for the strong TI, the SG is compatible with at most $N_t - 1$ independent weak TI phases.
 - [30] D. Varjas, F. de Juan, and Y.-M. Lu, ArXiv e-prints (2016), [arXiv:1603.04450](https://arxiv.org/abs/1603.04450).
 - [31] H. Watanabe, H. C. Po, A. Vishwanath, and M. P. Zaletel, *Proc. Natl. Acad. Sci. U.S.A.* **112**, 14551 (2015).
 - [32] H. Watanabe, H. C. Po, M. P. Zaletel, and A. Vishwanath, *Phys. Rev. Lett.* **117**, 096404 (2016).

- [33] L. Michel and J. Zak, *Phys. Rev. B* **59**, 5998 (1999).
- [34] L. Michel and J. Zak, *Euro Phys. Lett.* **50**, 519 (2000).
- [35] L. Michel and J. Zak, *Phys. Rep.* **341**, 377 (2001).
- [36] Note also that we have limited ourselves to the 230 SGs in this work, which only correspond to a subset of the 1651 magnetic SGs relevant for the study of magnetic materials. It is possible that new feQBIs will lie in this larger space of symmetry settings, which we will leave for future studies.
- [37] R. Chen, H. C. Po, J. B. Neaton, and A. Vishwanath, ArXiv e-prints (2016), [arXiv:1611.06860](https://arxiv.org/abs/1611.06860).

Appendix A: Review of symmetries in band structures

Here, we briefly review some notions and results concerning the consequences of symmetries on band structure. The discussion here will closely mirror that of the 1D example given in Sec. II, but we will assume a general 3D setting from the outset.

Consider a system of noninteracting fermions symmetric under a purely spatial symmetry group \mathcal{G} with the lattice translation subgroup T . An element $g \in \mathcal{G}$ that maps a point $\mathbf{x} \in \mathbb{R}^3$ to $g(\mathbf{x}) = p_g \mathbf{x} + \mathbf{t}_g \in \mathbb{R}^3$ may be characterized by an orthogonal matrix p_g and a vector \mathbf{t}_g . Thanks to the lattice translation T , it is natural to label the eigenenergy $E_m(\mathbf{k})$ by the band index m and the wavevector $\mathbf{k} \in \text{BZ}$. The notion of energy bands, however, becomes ambiguous whenever they cross, since the underlying wave function of a single band will generally become discontinuous. Instead, it is more natural to consider a set of entangled bands, separated from all others by band gaps above and below, as a single entity.

Whether a given set of energy bands can be isolated from the others dictate whether or not the system can be insulating, and therefore is a fundamental question in the study of electronic band structures. High-symmetry momenta play a crucial role in this analysis. The subgroup of \mathcal{G} that leaves a momentum $\mathbf{k} \in \text{BZ}$ invariant (up to a reciprocal lattice vector \mathbf{G}) is known as the ‘little group’ of \mathbf{k} , which is commonly denoted by $\mathcal{G}_{\mathbf{k}}$ [20]. As a set, we have

$$\mathcal{G}_{\mathbf{k}} = \{g \in \mathcal{G} : p_g \mathbf{k} = \mathbf{k} + \mathbf{G}\}. \quad (\text{A1})$$

By definition, lattice translations T automatically form a subgroup of $\mathcal{G}_{\mathbf{k}}$, and we say \mathbf{k} is a ‘high-symmetry momentum’ whenever $\mathcal{G}_{\mathbf{k}}$ contains any element aside from lattice translations. Note that when we say ‘all high-symmetry momenta’, we include all high-symmetry points, lines and planes in the BZ.

Generally, a spatial symmetry g demands $E_m(p_g \mathbf{k}) = E_m(\mathbf{k})$, and the corresponding wave functions are similarly related. When $g \in \mathcal{G}_{\mathbf{k}}$, the constraint becomes a local condition in momentum space. This implies the wave functions furnish a representation of $\mathcal{G}_{\mathbf{k}}$ [20]. Such representations encode the transformation properties of the BS at \mathbf{k} , and can be generally decomposed into a direct sum of ‘irreducible representations’ (irreps) $u_{\mathbf{k}}^{\alpha}$, which have been exhaustively tabulated in Ref. [20] for both spinless and spinful fermions. Insofar as symmetry properties are concerned, we can label a BS at \mathbf{k} by the set of non-negative integers

$$\{n_{\mathbf{k}}^{\alpha} : \alpha = 1, \dots, D_{\mathbf{k}}, \mathbf{k}: \text{high-symm. momentum}\}, \quad (\text{A2})$$

where $n_{\mathbf{k}}^{\alpha}$ denotes the number of times the α -th irrep appears in the BS, and $D_{\mathbf{k}}$ denotes the number of irreps. Note that such symmetry labeling makes no reference to the detailed energetics of the system, i.e. the labels are insensitive to the energetic arrangement of the individual bands within the BS.

A priori, a BS will carry independent symmetry labels $\{n_{\mathbf{k}}^{\alpha}\}$ and $\{n_{\mathbf{k}'}^{\beta}\}$ at distinct high-symmetry momenta \mathbf{k} and \mathbf{k}' . However, symmetries and continuity can cast extra constraints on such assignment [20]. To see this concretely, let

us introduce the notion of the Wyckoff positions in the momentum space. We group points in BZ based on their little group $\mathcal{G}_{\mathbf{k}}$. Namely, \mathbf{k}_1 and \mathbf{k}_2 belong to the same Wyckoff position iff there exists $g \in \mathcal{G}$ such that $\mathcal{G}_{\mathbf{k}_2} = g\mathcal{G}_{\mathbf{k}_1}g^{-1}$. For example, when \mathbf{k}_1 and \mathbf{k}_2 are related by $g_0 \in \mathcal{G}$, i.e., $\mathbf{k}_2 = p_{g_0} \mathbf{k}_1 + \mathbf{G}$, they belong to the same Wyckoff position as we have $\mathcal{G}_{\mathbf{k}_2} = g_0 \mathcal{G}_{\mathbf{k}_1} g_0^{-1}$. However, even when \mathbf{k}_1 and \mathbf{k}_2 are *not* related by symmetry, they might still belong to the same Wyckoff position. For example, imagine a line invariant under a n -fold rotation (or screw) C_n . Any point on this line (except for possibly the end points) has the identical little group generated by C_n and hence belong to the same Wyckoff position. Similar situation arises for a plane invariant under a mirror (or a glide). By assumption, the existence of band gaps imply the representation content of a BS is invariant within such high-symmetry lines or planes, and therefore it suffices to specify the representations at one arbitrarily chosen point of each Wyckoff position in the momentum space. Therefore, a full set of symmetry labels of a BS can be obtained by specifying only those arising from a finite number of representatives.

In addition, the BS is also labeled by the total number of bands in the BS, which we will denote by ν . Note that physically ν is simply the electron filling of the system when BS is interpreted as the set of filled bands in the full system. Aggregating all the labels $\{n_{\mathbf{k}}^{\alpha}\}$ and ν into a single quantity, we denote the representation content of a BS by \mathbf{n} , a set of D non-negative integers where $D = 1 + \sum_{\mathbf{k}} D_{\mathbf{k}}$. Here, we have chosen one arbitrary \mathbf{k} for each Wyckoff position in the momentum space, as explained above.

Now consider the reverse question: Given a symmetry setting, what is the set of admissible labels $\{\mathbf{n}\}$? To answer this, we introduce the notion of ‘compatibility relations.’ [20] For any pair of infinitesimally close momenta \mathbf{k} and $\mathbf{k} + \delta\mathbf{k}$, their little groups satisfy $\mathcal{G}_{\mathbf{k} + \delta\mathbf{k}} \leq \mathcal{G}_{\mathbf{k}}$ (assuming a proper choice of labeling for the two momenta). Since the irreps at the higher-symmetry momentum \mathbf{k} can be decomposed into those of the lower-symmetry ones at $\mathbf{k} + \delta\mathbf{k}$, the symmetry labels $\{n_{\mathbf{k} + \delta\mathbf{k}}^{\alpha}\}$ are fully constrained by $\{n_{\mathbf{k}}^{\beta}\}$. This is captured by the ‘compatibility relations’, one for each value of α ,

$$n_{\mathbf{k} + \delta\mathbf{k}}^{\alpha} = \sum_{\beta} c_{\alpha\beta}^{\mathbf{k}, \delta\mathbf{k}} n_{\mathbf{k}}^{\beta}, \quad (\text{A3})$$

where the coefficients $c_{\alpha\beta}^{\mathbf{k}, \delta\mathbf{k}}$ are non-negative integers. There is also a similar compatibility on the filling: $\nu = \sum_{\alpha} \dim[u_{\mathbf{k}}^{\alpha}] n_{\mathbf{k}}^{\alpha}$, where $\dim[u_{\mathbf{k}}^{\alpha}]$ denotes the dimension of the irrep α (i.e. the number of bands involved).

As our target is to study BSs as global entities, it is instructive to collect all compatibility relations into a system of linear equations:

$$\mathcal{C} \mathbf{n} = 0, \quad (\text{A4})$$

where \mathcal{C} is an integer-valued matrix with coefficients determined by those in Eq. (A3). By definition, any BS can be identified with an \mathbf{n} satisfying Eq. (A4). Conversely, any set of D non-negative integers $\mathbf{n} \in \mathbb{Z}_{\geq 0}^D$ satisfying Eq. (A4) can be identified with a physical band structure (Appendix D 2).

Appendix B: Atomic insulators as band structures

In Appendix A we characterized each BS by \mathbf{n} , the set of integers $n_{\mathbf{k}}^{\alpha}$ that specifies the representation contents of the BS. In this section, we derive a general formula that gives \mathbf{n} for each AI.

1. Regular representation

As a warm-up for a more group-theoretic discussion, let us revisit the regular representation of a finite group G . Here we label an element of the group by $i = 1, 2, \dots, |G|$. Take an abstract state $|0\rangle$ and generate other states by $|i\rangle = \hat{g}_i|0\rangle$. The action of symmetry $g_k \in G$ on $|i\rangle$ can be readily computed as

$$\hat{g}_k|i\rangle = \hat{g}_k(\hat{g}_i|0\rangle) = z_{k,i}(g_k \hat{g}_i)|0\rangle = \sum_j |j\rangle \delta_{g_j, g_k g_i} z_{k,i}. \quad (\text{B1})$$

Here we introduced a factor system z to include possible projective representations due to the spin degrees of freedom. This result suggests that $\{|i\rangle\}_{i=1}^{|G|}$ forms a basis of the so-called regular representation of G :

$$[U(g_k)]_{j,i} = \delta_{g_j, g_k g_i} z_{k,i}. \quad (\text{B2})$$

The most important property of this representation is that $\text{tr}[U(g_i)] = |G| \delta_{g_i, e}$ (e is the identity). From the orthogonality of the representation character, this means that U contains each irrep of G precisely d times, where d is the dimension of the irrep.

2. Wyckoff position and site symmetry representations

Now we move onto the representation contents of AIs. By definition, an AI is specified by (i) the location of the sites on which atomic orbitals sit and (ii) the type of orbitals on each site. Mathematically, these two inputs correspond to the choice of Wyckoff position (in the real space) and the representation of the site symmetry group of a site in the Wyckoff position.

Just as we defined the little group of \mathbf{k} , let us define the little group of \mathbf{x} as the subgroup of \mathcal{G} that leaves \mathbf{x} invariant. We call it the site symmetry group $\mathcal{G}_{\mathbf{x}}$ of \mathbf{x} . As a set, we have

$$\mathcal{G}_{\mathbf{x}} = \{h \in \mathcal{G} \mid h(\mathbf{x}) \equiv p_h \mathbf{x} + \mathbf{t}_h = \mathbf{x}\}. \quad (\text{B3})$$

Since the map $h \mapsto p_h$ is one-to-one for $h \in \mathcal{G}_{\mathbf{x}}$, we sometimes identify $h \in \mathcal{G}_{\mathbf{x}}$ with its point-group part p_h in the following. As before, two points \mathbf{x}_1 and \mathbf{x}_2 belong to the same Wyckoff position iff there exists $g \in \mathcal{G}$ such that $\mathcal{G}_{\mathbf{x}_2} = g \mathcal{G}_{\mathbf{x}_1} g^{-1}$. The full list of different Wyckoff positions (in the real space) is available in Ref. [28].

Let us pick a site \mathbf{x} in the unit cell UC. By definition, elements of \mathcal{G} not belonging to $\mathcal{G}_{\mathbf{x}}$ will move \mathbf{x} . The crystallographic orbit $\{g(\mathbf{x}) \mid g \in \mathcal{G}\}$ defines a \mathcal{G} -symmetric lattice $L_{\mathbf{x}}$. Let $\{\mathbf{x}_{\sigma}\}_{\sigma=1,2,\dots}$ ($\mathbf{x}_1 \equiv \mathbf{x}$) be the lattice points in UC.

We choose $\{g_{\sigma}\}_{\sigma=1,2,\dots}$ from \mathcal{G} in such a way that $g_{\sigma=1} = e$ ($e \in \mathcal{G}$ is the identity) and $g_{\sigma}(\mathbf{x}) = \mathbf{x}_{\sigma}$ for $\sigma = 2, 3, \dots$. Namely, $\{g_{\sigma}\}_{\sigma=1,2,\dots}$ is a complete set of representatives of $\mathcal{W}_{\mathbf{x}} \equiv (\mathcal{G}/\mathcal{G}_{\mathbf{x}})/T$.

We want to introduce an orbital on every site of $L_{\mathbf{x}}$ in a ‘symmetric’ manner. To that end, let us first put states $\{|\phi_{\mathbf{x},i,\mathbf{k}}^r\rangle\}_{i=1}^{\dim[u_{\mathbf{x}}^r]}$ on \mathbf{x} that obey an irreps $u_{\mathbf{x}}^r$ of $\mathcal{G}_{\mathbf{x}}$:

$$u_{\mathbf{x}}^r(p_h)u_{\mathbf{x}}^r(p_{h'}) = z_{p_h, p_{h'}}u_{\mathbf{x}}^r(p_h p_{h'}), \quad (\text{B4})$$

$$\hat{h}|\phi_{\mathbf{x},i,\mathbf{k}}^r\rangle = \sum_j |\phi_{\mathbf{x},j,p_h \mathbf{k}}^r\rangle [u_{\mathbf{x}}^r(p_h)]_{ji}, \quad (\text{B5})$$

$$\hat{h}(\hat{h}'|\phi_{\mathbf{x},i,\mathbf{k}}^r\rangle) = z_{p_h, p_{h'}}(\hat{h}\hat{h}')|\phi_{\mathbf{x},i,\mathbf{k}}^r\rangle \quad (\text{B6})$$

for $h, h' \in \mathcal{G}_{\mathbf{x}}$ and

$$\hat{\mathbf{t}}_{\mathbf{R}}|\phi_{\mathbf{x},i,\mathbf{k}}^r\rangle = |\phi_{\mathbf{x},i,\mathbf{k}}^r\rangle e^{-i\mathbf{k}\cdot\mathbf{R}} \quad (\text{B7})$$

for $\mathbf{t}_{\mathbf{R}} \in T$. The orbitals at other sites of $L_{\mathbf{x}}$ are then defined by $|\phi_{\mathbf{x}_{\sigma},i,\mathbf{k}}^r\rangle \equiv \hat{g}_{\sigma}|\phi_{\mathbf{x},i,p_{\sigma}^{-1}\mathbf{k}}^r\rangle$. In these expressions, $z_{p_h, p_{h'}}$ is a factor system of the projective representation originating from the spin degrees of freedom. For spinless fermions one should simply set $z_{p_h, p_{h'}} = 1$.

The choice of the position \mathbf{x} to start with and the choice of an irrep $u_{\mathbf{x}}^r$ of the site symmetry group $\mathcal{G}_{\mathbf{x}}$ will specify the AI and its representation contents as we will see now.

3. Representation contents of an AI

To determine the transformation of $\{|\phi_{\mathbf{x}_{\sigma},i,\mathbf{k}}^r\rangle\}_{\sigma,i,\mathbf{k}}$ under \mathcal{G} , note that any element $g \in \mathcal{G}$ can be uniquely decomposed as $g = t_{\mathbf{R}} g_{\sigma} h$ where $t_{\mathbf{R}} \in T$ and $h \in \mathcal{G}_{\mathbf{x}}$. In particular, we can decompose $g g_{\sigma}$ as $t_{\mathbf{R}} g_{\sigma'} h$ with $\mathbf{R} = p_g \mathbf{x}_{\sigma} + \mathbf{t}_g - \mathbf{x}_{\sigma'}$. Therefore,

$$\begin{aligned} & \hat{g}|\phi_{\mathbf{x}_{\sigma},i,\mathbf{k}}^r\rangle \\ &= z_{p_g, p_{\sigma}}(g \hat{g}_{\sigma})|\phi_{\mathbf{x},i,p_{\sigma}^{-1}\mathbf{k}}^r\rangle \\ &= z_{p_g, p_{\sigma}}(t_{\mathbf{R}} \hat{g}_{\sigma'} h)|\phi_{\mathbf{x},i,p_{\sigma}^{-1}\mathbf{k}}^r\rangle \\ &= \frac{z_{p_g, p_{\sigma}}}{z_{p_{\sigma'}, p_h}} \hat{\mathbf{t}}_{\mathbf{R}} \hat{g}_{\sigma'}(\hat{h}|\phi_{\mathbf{x},i,p_{\sigma}^{-1}\mathbf{k}}^r\rangle) \\ &= \frac{z_{p_g, p_{\sigma}}}{z_{p_{\sigma'}, p_h}} \sum_{i'} (\hat{\mathbf{t}}_{\mathbf{R}}|\phi_{\mathbf{x}_{\sigma'},i',p_g \mathbf{k}}^r\rangle) [u_{\mathbf{x}}^r(p_h)]_{i'i} \\ &= \sum_{\sigma', i', \mathbf{k}'} |\phi_{\mathbf{x}_{\sigma'},i',\mathbf{k}'}^r\rangle [U_{\mathbf{x}}^r(g)]_{\sigma' i' \mathbf{k}' \sigma i \mathbf{k}}, \end{aligned} \quad (\text{B8})$$

where

$$\begin{aligned} [U_{\mathbf{x}}^r(g)]_{\sigma' i' \mathbf{k}' \sigma i \mathbf{k}} &= \delta'_{\mathbf{x}_{\sigma'}, p_g \mathbf{x}_{\sigma} + \mathbf{t}_g} \delta''_{\mathbf{k}', p_g \mathbf{k}} e^{-i\mathbf{k}' \cdot (p_g \mathbf{x}_{\sigma} + \mathbf{t}_g - \mathbf{x}_{\sigma'})} \\ &\quad \times \frac{z_{p_g, p_{\sigma}}}{z_{p_{\sigma'}, p_{\sigma}^{-1} p_g p_{\sigma}}} [u_{\mathbf{x}}^r(p_{\sigma}^{-1} p_g p_{\sigma})]_{i'i}. \end{aligned} \quad (\text{B9})$$

Namely, an AI constructed from an irrep $u_{\mathbf{x}}^r$ of $\mathcal{G}_{\mathbf{x}}$ has a (generically reducible) representation $U_{\mathbf{x}}^r$ of \mathcal{G} . In this equation, $\delta'_{\mathbf{x}_1, \mathbf{x}_2} = 1$ only when $\mathbf{x}_1 = \mathbf{x}_2$ modulo a lattice vector. Similarly, $\delta''_{\mathbf{k}_1, \mathbf{k}_2} = 1$ only when $\mathbf{k}_1 = \mathbf{k}_2$ modulo a reciprocal lattice vector.

Let us focus on a particular \mathbf{k} in BZ and let $\mathcal{G}_{\mathbf{k}}$ be the little group. The representation of $\mathcal{G}_{\mathbf{k}}$ of the AI is immediately given by $U_{\mathbf{x}}^r$ by restricting \mathcal{G} to $\mathcal{G}_{\mathbf{k}}$. In particular, its character is

$$\begin{aligned} \chi_{\mathbf{x},\mathbf{k}}^r(g) &\equiv \text{tr}[U_{\mathbf{x}}^r(g)] \\ &= \sum_{\sigma=1}^{|\mathcal{W}_{\mathbf{x}}|} \delta'_{\mathbf{x}\sigma, p_g \mathbf{x}\sigma + \mathbf{t}_g} e^{-i\mathbf{k}\cdot(p_g \mathbf{x}\sigma + \mathbf{t}_g - \mathbf{x}\sigma)} \\ &\quad \times \frac{z_{p_g, p_\sigma}}{z_{p_\sigma, p_\sigma^{-1} p_g p_\sigma}} \chi_{\mathbf{x}}^r(p_\sigma^{-1} p_g p_\sigma), \end{aligned} \quad (\text{B10})$$

where $\chi_{\mathbf{x}}^r(p_h) \equiv \text{tr}[u_{\mathbf{x}}^r(p_h)]$. Note that this result does not depend on the choice of \mathbf{x}_σ ; even if one chose $\mathbf{x}'_\sigma = \mathbf{x}_\sigma + \mathbf{R}_\sigma$ instead, the character is unchanged.

Let $u_{\mathbf{k}}^\alpha$'s be irreps of $\mathcal{G}_{\mathbf{k}}$ and $\chi_{\mathbf{k}}^\alpha(g) = \text{tr}[u_{\mathbf{k}}^\alpha(g)]$ be their characters. Then, the irrep $u_{\mathbf{k}}^\alpha$ appears in $U_{\mathbf{x}}^r(g)$

$$n_{\mathbf{k}}^\alpha = \sum_{g \in \mathcal{G}_{\mathbf{k}}/T} \frac{1}{|\mathcal{G}_{\mathbf{k}}/T|} [\chi_{\mathbf{k}}^\alpha(g)]^* \chi_{\mathbf{x},\mathbf{k}}^r(g) \in \mathbb{Z} \quad (\text{B11})$$

times. This is the formula that gives n for a AI in general.

4. The general position

As a special case of the above general discussion, let us assume that the site symmetry group $\mathcal{G}_{\mathbf{x}}$ is trivial, i.e., $\mathcal{G}_{\mathbf{x}} = \{e\}$. In other words, let us assume that \mathbf{x} belongs to the general Wyckoff position. There is only one trivial representation $u_{\mathbf{x}}^{r=1}(e) = 1$ for such a generic position. In this case, Eq. (B10) reduces to

$$\chi_{\mathbf{x},\mathbf{k}}^{r=1}(g) = |\mathcal{G}/T| \delta_{g,e}. \quad (\text{B12})$$

Therefore, using $\chi_{\mathbf{k}}^\alpha(e) = \text{tr}[u_{\mathbf{k}}^\alpha(e)] = \dim[u_{\mathbf{k}}^\alpha]$, we get

$$n_{\mathbf{k}}^\alpha|_{\text{generic position}} = \frac{|\mathcal{G}/T|}{|\mathcal{G}_{\mathbf{k}}/T|} \dim[u_{\mathbf{k}}^\alpha] > 0. \quad (\text{B13})$$

This results means that the AI constructed from the trivial orbital on a generic position \mathbf{x} contains every irrep $u_{\mathbf{k}}^\alpha$ at least once at each \mathbf{k} .

5. The special position

Next, consider a position \mathbf{x} with a nontrivial $\mathcal{G}_{\mathbf{x}} > e$. In other words, \mathbf{x} belongs to a special Wyckoff position. In this case, there are several irreps $u_{\mathbf{x}}^r$. We have a sum-rule separately for each \mathbf{x} :

$$n_{\mathbf{k}}^\alpha|_{\text{generic position}} = \sum_{r: \text{all irreps on } \mathbf{x}} \dim[u_{\mathbf{x}}^r] n_{\mathbf{k}}^\alpha|_{\text{irrep } u_{\mathbf{x}}^r \text{ on } \mathbf{x}}. \quad (\text{B14})$$

6. TR invariant AIs

To construct a TR invariant AI, we have to determine if the time-reversal (TR) symmetry T with $\hat{T}^2 = (-1)^N$ ($N = 1$ for the spinful case and $N = 0$ for the spinless case) enhances the degeneracy of the irrep $u_{\mathbf{x}}^r$. As we will explain in Appendix C, there is an easy way to do so using the character $\chi_{\mathbf{x}}^r(h) \equiv \text{tr}[u_{\mathbf{x}}^r(h)]$ of $h \in \mathcal{G}_{\mathbf{x}}$. As we explain the detailed discussion in Appendix C, here we only summarize the result.

To determine the the consequence of the TR symmetry, one should compute the sum $\frac{1}{|\mathcal{G}_{\mathbf{x}}|} \sum_{h \in \mathcal{G}_{\mathbf{x}}} z_{p_h, p_h} \chi_{\mathbf{x}}^r(h^2)$, which can be either $+1$, 0 , or -1 . Then,

$$\begin{aligned} &\frac{1}{|\mathcal{G}_{\mathbf{x}}|} \sum_{h \in \mathcal{G}_{\mathbf{x}}} z_{p_h, p_h} \chi_{\mathbf{x}}^r(h^2) \\ &= \begin{cases} +(-1)^N & : u_{\mathbf{x}}^r \text{ by itself is TR invariant.} \\ -(-1)^N & : \text{Two } u_{\mathbf{x}}^r \text{'s are paired under TR.} \\ 0 & : u_{\mathbf{x}}^r \text{ and } (u_{\mathbf{x}}^r)^* \text{ are different and are paired.} \end{cases} \end{aligned} \quad (\text{B15})$$

Namely, if the sum is either $-(-1)^N$ or 0 , the AI constructed from the irrep $u_{\mathbf{x}}^r$ on the site \mathbf{x} alone is not TR symmetric, and one has to make a proper stacking with its TR pair.

7. Uniform basis

In Appendix B 3, we constructed a representation $U_{\mathbf{x}}^r$ of \mathcal{G} starting from an irrep $u_{\mathbf{x}}^r$ of $\mathcal{G}_{\mathbf{x}}$. There is yet another construction of a representation of \mathcal{G} . Suppose that we know a representation $u(p_g)$ of the point group \mathcal{G}/T . Then a representation of \mathcal{G} is given by

$$\begin{aligned} [U(g)]_{\sigma' i' \mathbf{k}', \sigma i \mathbf{k}} &= \delta'_{\mathbf{x}\sigma', p_g \mathbf{x}\sigma + \mathbf{t}_g} \delta''_{\mathbf{k}', p_g \mathbf{k}} \\ &\quad \times e^{-i\mathbf{k}'\cdot(p_g \mathbf{x}\sigma + \mathbf{t}_g - \mathbf{x}\sigma')} [u(p_g)]_{i' i} \end{aligned} \quad (\text{B16})$$

The advantage of this representation is that we have the same representation $u(p_g)$ on every site. As a result, the effect of spin-orbit coupling, for example, can be interpreted much easily than $U_{\mathbf{x}}^r$. Our leSM example discussed in detail in Appendix F 1 is formulated using this representation. The drawback is that this construction generally requires as input particular representations of $\mathcal{G}_{\mathbf{x}}$, in contrast to the construction in Appendix B 3 which applies to any representation, in particular also the irreducible ones.

Appendix C: Time-reversal symmetry

In this Appendix, we will follow the discussion in Ref. [20] on the consequence of the TR symmetry T commuting with every element of G . We will write $\hat{T}^2 = (-1)^N$ where $N = 1$ for the spinful case and $N = 0$ for the spinless case.

1. General case

Let us start with a finite group G in general. Suppose that $\{|i\rangle\}_{i=1}^d$ ($d \equiv \dim[u]$) is a basis of an irrep u of G :

$$\hat{g}|i\rangle = |j\rangle u_{ji}(g). \quad (\text{C1})$$

Then $\{\hat{T}|i\rangle\}_{i=1}^d$ is a basis of the conjugate representation $u^*(g)$:

$$\hat{g}(\hat{T}|i\rangle) = (\hat{T}|j\rangle) u_{ji}^*(g). \quad (\text{C2})$$

When u and u^* are different irreps, the group $G \times \mathbb{Z}_2^T$ is simply represented by

$$D(g) = \begin{pmatrix} u & 0 \\ 0 & u^* \end{pmatrix}, \quad D(T) = \begin{pmatrix} 0 & (-1)^N \\ 1 & 0 \end{pmatrix}. \quad (\text{C3})$$

Thus in the following we will assume that u and u^* are the same irrep, i.e., $u^*(g) = v^\dagger u(g) v$ for a unitary matrix v . Using the definition of v twice, we have $(vv^*)u(g) = u(g)(vv^*)$ for every g . Since u is irreducible, we see $vv^* = \xi \mathbb{1}_d$ for $\xi = \pm 1$.

It is easy to see that the combination $|\bar{i}\rangle \equiv (\hat{T}|j\rangle) v_{ji}^\dagger$ transforms in the same way as $|i\rangle$:

$$\hat{g}|\bar{i}\rangle = |\bar{j}\rangle u_{ji}(g). \quad (\text{C4})$$

Hence the question is if $|i\rangle$ and $|\bar{i}\rangle$ are the same. To see this, we evaluate the inner-product $G_{ij} \equiv \langle i | \bar{j} \rangle$. Since \hat{g} is unitary, we have

$$G_{ij} = \langle i | \bar{j} \rangle = \langle \hat{g}|i\rangle, \hat{g}|\bar{j}\rangle = [u(g)^\dagger G u(g)]_{ij}, \quad (\text{C5})$$

i.e., G and $u(g)$ commute for every g . Since u is irreducible, we must have $G = c \mathbb{1}_d$. To compute c , note that

$$\hat{T}|i\rangle = |\bar{j}\rangle v_{ji}, \quad (\text{C6})$$

$$\hat{T}|\bar{i}\rangle = (-1)^N |j\rangle (v_{ji}^\dagger)^* = \xi (-1)^N |j\rangle v_{ji}. \quad (\text{C7})$$

The second line follows from the first by applying \hat{T} and using $v^T = \xi v$. Hence

$$\begin{aligned} c &= \frac{1}{d} \sum_{i=1}^d \langle i | \bar{i} \rangle = \frac{1}{d} \sum_{i=1}^d \langle \hat{T}|\bar{i}\rangle, \hat{T}|i\rangle \\ &= \frac{\xi (-1)^N}{d} (vv^\dagger)_{j,j'} \langle j' | \bar{j} \rangle = \xi (-1)^N c. \end{aligned} \quad (\text{C8})$$

Namely, when $\xi(-1)^N = -1$, c vanishes and $\{|i\rangle\}_{i=1}^d$ and $\{\hat{T}|i\rangle\}_{i=1}^d$ are orthogonal. On the other hand, when $\xi(-1)^N = 1$, c is finite and $\{|i\rangle\}_{i=1}^d$ and $\{\hat{T}|i\rangle\}_{i=1}^d$ are the same state.

To compute ξ from the character $\chi(g) = \text{tr}[u(g)]$, we note that

$$\begin{aligned} \omega_{g,g} u(g^2) &= u(g) u(g) = [u^*(g)]^* u(g) \\ &= [v^\dagger u(g) v]^* u(g) = \xi v u^*(g) v^* u(g). \end{aligned} \quad (\text{C9})$$

Therefore,

$$\begin{aligned} \frac{1}{|G|} \sum_g \omega_{g,g} \chi(g^2) &= \xi \frac{1}{|G|} \sum_g v_{ij} u_{jk}^*(g) v_{kl}^* u_{li}(g) \\ &= \xi \frac{1}{d} (vv^\dagger)_{i,i} = \xi. \end{aligned} \quad (\text{C10})$$

where, in the second last line we used the orthogonality of irreps $\sum_g u_{ij}^{(\alpha)}(g) u_{kl}^{(\beta)}(g)^* = (|G|/d) \delta_{ik} \delta_{jl} \delta^{\alpha\beta}$. From this orthogonality, it is also clear that $\sum_g \omega_{g,g} \chi(g^2) = 0$ when u and u^* are different irreps.

To summarize, to see if the TR symmetry changes of degeneracy for the irrep u of G , one should compute

$$\begin{aligned} &\frac{1}{|G|} \sum_g \omega_{g,g} \chi(g^2) \\ &= \begin{cases} +(-1)^N & : \text{Degeneracy is unchanged.} \\ -(-1)^N & : \text{Two } u\text{'s are paired under TR.} \\ 0 & : u \text{ and } u^* \text{ are different and are paired.} \end{cases} \end{aligned} \quad (\text{C11})$$

This is called Wigner's test in the literature [20].

2. Little group \mathcal{G}_k

Let us apply this method to the irrep \tilde{u}_k^α of \mathcal{G}_k/T . If there is no element $g \in \mathcal{G}$ such that $p_g \mathbf{k} = -\mathbf{k}$ modulo a reciprocal lattice vector \mathbf{G} , then the TR symmetry just implies an additional degeneracy between \tilde{u}_k^α and $\tilde{u}_{-\mathbf{k}}^\alpha$ and this case is easily handled. Thus, suppose that there is at least one $g \in \mathcal{G}$ such that $p_g \mathbf{k} = -\mathbf{k} + \mathbf{G}$.

An irrep \tilde{u}_k^α of \mathcal{G}_k/T gives an irrep $u_k^\alpha(p_h) = \tilde{u}_k^\alpha(p_h) e^{-i\mathbf{k} \cdot \mathbf{t}_h}$ of \mathcal{G}_k . It further induces an irrep $U^\alpha(g)$ of \mathcal{G} :

$$[U^\alpha(g)]_{\sigma',j,\sigma,i} = \sum_{h \in \mathcal{G}_k} \delta_{g g_\sigma, g_\sigma' h} \frac{z_{p_g, p_\sigma}}{z_{p_\sigma', p_h}} [u_k^\alpha(p_h)]_{ji}. \quad (\text{C12})$$

Here, $\{g_\sigma\}_{\sigma=1}^{|\mathcal{G}/\mathcal{G}_k|}$ ($g_{\sigma=1} = e$) is a complete set of representative of $\mathcal{G}/\mathcal{G}_k$. Namely, the set of $\mathbf{k}_\sigma \equiv p_\sigma \mathbf{k}$ forms the star of \mathbf{k} . Then

$$\begin{aligned} \text{tr}[U^\alpha(g)] &= \sum_\sigma \sum_{h \in \mathcal{G}_k} \delta_{g, g_\sigma h g_\sigma^{-1}} \frac{z_{p_g, p_\sigma}}{z_{p_\sigma, p_h}} \text{tr}[u_k^\alpha(p_h)] \\ &= \sum_\sigma \sum_{h \in \mathcal{G}_k} \delta_{g, h} \text{tr}[u_{\mathbf{k}_\sigma}^\alpha(p_h)], \end{aligned} \quad (\text{C13})$$

where $u_{\mathbf{k}_\sigma}^\alpha(p_h) = \frac{z_{p_h, p_\sigma}}{z_{p_\sigma, p_\sigma^{-1} p_h p_\sigma}} u_k^\alpha(p_\sigma^{-1} p_h p_\sigma)$. Hence,

$$\begin{aligned} &\frac{1}{|G|} \sum_{g \in \mathcal{G}} z_{p_g, p_g} \text{tr}[U^\alpha(g^2)] \\ &= \frac{1}{|G|} \sum_\sigma \sum_{g \in \mathcal{G}} \sum_{h \in \mathcal{G}_k} \delta_{g^2, h} z_{p_g, p_g} \tilde{\chi}_{\mathbf{k}_\sigma}^\alpha(p_h) e^{-i\mathbf{k}_\sigma \cdot \mathbf{t}_h} \\ &= \frac{1}{|G_k|} \sum_{g \in \mathcal{G}} \sum_{h \in \mathcal{G}_k} \delta_{g^2, h} z_{p_g, p_g} \tilde{\chi}_{\mathbf{k}}^\alpha(p_{g^2}) e^{-i\mathbf{k} \cdot (p_g \mathbf{t}_g + \mathbf{t}_g)} \\ &= \frac{1}{|G_k/T|} \sum_{g \in G_k/T} \delta_{p_g \mathbf{k}, -\mathbf{k}} z_{p_g, p_g} \tilde{\chi}_{\mathbf{k}}^\alpha(p_{g^2}) e^{-i\mathbf{k} \cdot (p_g \mathbf{t}_g + \mathbf{t}_g)} \end{aligned}$$

where $\tilde{\chi}_{\mathbf{k}}^\alpha(p_h) = \text{tr}[\tilde{u}_{\mathbf{k}}^\alpha(p_h)] = \text{tr}[u_{\mathbf{k}}^\alpha(p_h) e^{i\mathbf{k} \cdot \mathbf{t}_h}]$ and z_{p_g, p_g} is the projective factor arising from the spin. To go to the third line, we used the fact that contributions from each star

of \mathbf{k} are identical and replaced \sum_{σ} by the factor $|\mathcal{G}|/|\mathcal{G}_{\mathbf{k}}|$. To go to the last line, we performed the sum over the translation subgroup T , which results in the constraints $p_g \mathbf{k} = -\mathbf{k} + \exists \mathbf{G}$ because $e^{-i\mathbf{k} \cdot (p_g \mathbf{R} + \mathbf{R})} = e^{-i(\mathbf{k} + p_g^{-1} \mathbf{k}) \cdot \mathbf{R}} = 1$. Therefore, we have [20]

$$\begin{aligned} & \frac{1}{|\mathcal{G}_{\mathbf{k}}/T|} \sum_{g \in \mathcal{G}_{\mathbf{k}}/T} \delta''_{p_g \mathbf{k}, -\mathbf{k}} z_{p_g, p_g} \tilde{\chi}_{\mathbf{k}}^{\alpha}(p_g^2) e^{-i\mathbf{k} \cdot (p_g \mathbf{t}_g + \mathbf{t}_g)} \quad (\text{C14}) \\ & = \begin{cases} +(-1)^N & : \text{Degeneracy is unchanged.} \\ -(-1)^N & : \text{Two } u_{\mathbf{k}}^{\alpha} \text{'s are paired under TR.} \\ 0 & : u_{\mathbf{k}}^{\alpha} \text{ is paired with another irrep } u_{\mathbf{k}}^{\beta}. \end{cases} \quad (\text{C15}) \end{aligned}$$

As explained in the main text, when an irrep $u_{\mathbf{k}}^{\alpha}$ is paired with a different irrep $u_{\mathbf{k}}^{\beta}$ under TR, we simply add to \mathcal{C} an additional compatibility relation $n_{\mathbf{k}}^{\alpha} = n_{\mathbf{k}}^{\beta}$; when $u_{\mathbf{k}}^{\alpha}$ is paired with itself, we demand $n_{\mathbf{k}}^{\alpha}$ to be an even integer, which can be achieved by redefining $\tilde{n}_{\mathbf{k}}^{\alpha} \equiv n_{\mathbf{k}}^{\alpha}/2$ and a corresponding rewriting of \mathcal{C} in terms of $\tilde{\mathbf{n}}$.

Appendix D: Structure of {BS} and computation of X_{BS}

1. Mathematical details

Here, we discuss some relatively formal aspects of our mathematical framework. We will start with the claim

$$\{\text{BS}\} \equiv \ker \mathcal{C} \cap \mathbb{Z}^D \Rightarrow \{\text{BS}\} \simeq \mathbb{Z}^{d_{\text{BS}}}, \quad (\text{D1})$$

where $d_{\text{BS}} \equiv \dim \ker \mathcal{C}$. This claim can be interpreted geometrically: Embedded in \mathbb{R}^D , \mathbb{Z}^D is a hypercubic lattice and $\ker \mathcal{C}$ defines a d_{BS} -dimensional hyperplane. $\{\text{BS}\}$ is then the collection of lattice sites ‘sliced’ by $\ker \mathcal{C}$, which defines a Bravais lattice in d_{BS} dimensions.

Alternatively, this can also be understood algebraically, as we now discuss in details. First observe $\{\text{BS}\} \leq \mathbb{Z}^D$. Since any subgroup of a finitely generated abelian group is again finitely generated, and that no element in \mathbb{Z}^D has finite order, we see that $\{\text{BS}\} \simeq \mathbb{Z}^d$ for some $d \leq D$. Next, note that as \mathcal{C} is a matrix of integer coefficients, its solution space can be identified as a vector subspace of \mathbb{Q}^D (instead of \mathbb{R}^D). Let $\{\mathbf{q}_i : i = 1, \dots, d_{\text{BS}}\}$ be any complete basis for $\ker \mathcal{C} \simeq \mathbb{Q}^{d_{\text{BS}}}$. Since only a finite number of rational numbers are involved, we can always multiply the basis by the least-common multiple of all the denominators to arrive at an integer-valued basis. This implies $\{\text{BS}\}$ has at least d_{BS} linearly-independent elements, i.e. $d \geq d_{\text{BS}}$. Now also observe that as $\{\text{BS}\} \leq \ker \mathcal{C}$, $\ker \mathcal{C}$ has at least d linearly-independent vectors, which implies $d_{\text{BS}} \leq d \leq d_{\text{BS}}$.

Next we discuss the computation of $X_{\text{BS}} \equiv \{\text{BS}\}/\{\text{AI}\}$, where $\{\text{AI}\} \simeq \mathbb{Z}^{d_{\text{AI}}} \leq \{\text{BS}\}$ denotes the subgroup of BS arising from AIs. The first step in the analysis is to compare their ranks. d_{BS} , a property of \mathcal{C} , is determined once all compatibility relations are found. d_{AI} can be computed as follows: Any AI can be understood as a stack of those arising from fully occupying an irrep of the site-symmetry group of a Wyckoff

position. Hence, by focusing on the finite number of AIs arising from these irreps, we can find a (generally over-complete) basis for $\{\text{AI}\}$ using the formalism developed in Appendices B and C. Finally we simply extract the number of linearly independent combinations among them, which is by definition d_{AI} .

Generally, we have $d_{\text{AI}} \leq d_{\text{BS}}$, and the general structure of the quotient group is given by

$$X_{\text{BS}} = \mathbb{Z}^{d_{\text{BS}} - d_{\text{AI}}} \times \mathbb{Z}_{s_1} \times \mathbb{Z}_{s_2} \times \dots \times \mathbb{Z}_{s_{d_{\text{AI}}}}. \quad (\text{D2})$$

It remains to compute the integers $s_i \geq 1$. In more physical terms, any element of X_{BS} corresponds to a class of BSs that cannot be obtained from integer combinations (i.e. stacking) of entries in $\{\text{AI}\}$. Now consider a $\mathbf{b} \in \{\text{BS}\}$ with its equivalence class $[\mathbf{b}]$ being the generator of a factor Z_{s_i} in X_{BS} . From definition, $s_i[\mathbf{b}] = [s_i \mathbf{b}]$ is the trivial element of X_{BS} , i.e. $s_i \mathbf{b}$ is an AI. Running the argument in reverse, the torsion (i.e. finite-order) elements of X_{BS} correspond to (the classes of) fractions of AIs that are nonetheless in $\{\text{BS}\}$, and hence to compute the s_i 's in Eq. (D2) one simply studies the possible set of coefficients for which $\sum_{i=1}^{d_{\text{AI}}} q_i \mathbf{a}_i$, $q_i \in \mathbb{Q}$, is integer-valued. This can be readily computed using the ‘Smith normal form’, which is, loosely speaking, an integer-valued version of the singular-value decomposition (in our context).

An interesting observation is that, for all the 230×4 cases we studied, corresponding to all the SGs assuming spinless or spinful fermions with or without TR symmetry, we found $d_{\text{BS}} = d_{\text{AI}}$. This implies a basis for $\{\text{BS}\}$ can be obtained by a suitable combination of the basis of $\{\text{AI}\}$ using rational coefficients, which are found in the computation of s_i described above. Equivalently, we found that a BS can always be ‘expanded’ as

$$\text{BS} = \sum_{\mathbf{x}} \sum_r q_{\mathbf{x},r} \mathbf{n}_{\mathbf{x},r}, \quad (\text{D3})$$

where $\mathbf{n}_{\mathbf{x},r}$ denotes the \mathbf{n} of the AI arising from fully occupying a site-symmetry group irrep $u_{\mathbf{x}}^r$ of the position \mathbf{x} (it is sufficient to choose one representative of \mathbf{x} for each Wyckoff position), and $q_{\mathbf{x},r} \in \mathbb{Q}$ are rational numbers. This is very similar to the decomposition of energy bands at high-symmetry momenta into irreps of the little group, except that this is now performed in a global manner over the BZ. An interesting open question is whether there is any symmetry setting, say when one studies the remaining magnetic SGs, for which $d_{\text{BS}} > d_{\text{AI}}$ and therefore leads to an infinite X_{BS} (i.e. some BSs remain non-atomic no matter how many copies we take). Alternatively, if such equality always holds for any symmetry settings, there should be a more elegant method to prove that X_{BS} is always finite.

In closing, we comment that the expansion in Eq. (D3) is similar in spirit to the notion of ‘elementary energy bands’ developed in a series of work by Refs. [33–35]. In our language, these earlier results focus on such a decomposition between the AIs, and whether or not the building blocks of such decomposition, dubbed ‘elementary energy bands’, can be ‘split’ into energy bands of lower fillings. These earlier works approached the problem from a real-space perspective,

which in our language is about the structure of $\{\text{AI}\}$. In contrast, our formalism, centered on the structure of $\{\text{BS}\}$, automatically captures all the momentum-space constraints and is more suited for studying topological band structures: our notion of a global decomposition allows for ‘quantum interference in momentum space’, which is more general than that in Refs. [33–35]. Finally, we also remark that the results concerning ‘energy band connectivity’ in Refs. [33–35]. has interesting implications on finding leSMs (specifically, for spinless fermions with TR symmetry).

(Note: From a more mathematical perspective, the earlier results in Refs. [33–35] are concerned with a decomposition in terms of the direct sum \oplus , whereas we have first made a generalization $\oplus \rightarrow +$, akin to how representation rings are constructed, and then further assert that the decomposition is physically meaningful with rational coefficients, as long as the resulting (formal) sum lies in $\{\text{BS}\}$.)

2. Physical relevance of X_{BS}

Having discussed the mathematical aspect of the formalism, we now comment on why such notions are relevant to physical band structures. Recall we have motivated the definition of $\{\text{BS}\}$ by asserting that, as long as only symmetry properties are concerned, a set of energy bands can be labelled simply by a count of the multiplicities of each irrep at the high-symmetry momenta. A priori, it is insensible to say that an irrep appears a ‘negative number of times’. As mentioned in the main text, this leads to an additional condition in connecting the entries of $\{\text{BS}\}$ to physical band structures—for $\mathbf{n} \in \{\text{BS}\}$ to be physical, all components of \mathbf{n} must be non-negative. Equivalently, one can define a ‘physical subset’

$$\{\text{BS}\}_{\text{P}} \equiv \{\text{BS}\} \cap \mathbb{Z}_{\geq 0}^D \subset \{\text{BS}\}. \quad (\text{D4})$$

As we have explained, all elements in $\{\text{BS}\}_{\text{P}}$ enjoy the properties of a general element in $\{\text{BS}\}$, say the decomposition in Eq. (D3). Therefore, the inclusion of unphysical entries, crucial for the group properties of $\{\text{BS}\}$, should be viewed merely as a mathematical way to simplify the analysis of the physical problem. (If one insists, one can identify $\{\text{BS}\}_{\text{P}}$ as a commutative monoid enjoying similar properties as the group $\{\text{BS}\}$. However, we do not find this perspective particularly useful in our discussion, and would rather stick with $\{\text{BS}\}$, a simpler mathematical gadget.)

However, there are still two questions we have to address in order to quantify the relevance of our mathematical framework to the study of real, physical band structures:

- (1) Do all entries of $\{\text{BS}\}_{\text{P}}$ correspond to physically realizable band structures?
- (2) Do all nontrivial classes in X_{BS} have physical representatives?

To answer (1), we consider an arbitrary element of $\{\text{BS}\}_{\text{P}}$, and let a set of physical bands possess the desired irrep content at all high-symmetry momentum points. (If only high-symmetry lines or planes are present, we choose arbitrary,

isolated representatives.) This is always possible by a suitable arrangement of the energies of the irreps at these isolated momentum points. By symmetries and continuity, all compatibility relations are locally satisfied near these points. Suppose there are still certain band crossings obstructing us from identifying this set of bands as a BS. Since any pair of bands carrying the same symmetry representation will generically anti-cross, these band crossings must correspond to an ‘exchange of irreps’ between our target set of bands and the others. As all compatibility relations are globally satisfied by assumption, such exchange must be accidental in nature, i.e. it is possible to perturb the Hamiltonian in a symmetric fashion to get rid of all the band crossings. This then leads to a BS corresponding to the specified element in $\{\text{BS}\}_{\text{P}}$.

Note that, however, there is a subtlety in the statement on ‘generic anti-crossing’: Topological band degeneracies, like Weyl points, can only be ‘pushed away’ but not lifted, unless their topological charges are neutralized by their partners. This does not concern us, since by our definition of BS we will only be interested in band gaps at high-symmetry momenta, and therefore as long as these degeneracies can be moved away they do not affect our discussion. This also explains why the notion of reSM, which *cannot* be insulating due to the specified representation content, is still consistent with our notion of BS.

To address (2), we let \mathbf{b} be a representative of a nontrivial class in X_{BS} which is not physical, i.e. certain entries in \mathbf{b} are negative. Now, we consider a small corollary from Appendix B 4: all irreps appear at least once in the AI corresponding to the generic Wyckoff position [see Eq. (B13)]. Therefore, we can always stack \mathbf{b} with a sufficiently large number of copies of the generic AI and rectify the representation content. By definition, such stacking leads to a physical BS belonging to the same nontrivial class as \mathbf{b} , and hence all classes of X_{BS} have physical representatives.

Appendix E: reQBI and reSM

1. Relationship

As we have discussed in the main text, our notion of a BS is compatible with both band insulators and semimetals, as long as a continuous band gap is sustained at all high-symmetry momenta. In particular, the nontrivial entries in X_{BS} can sometimes correspond to reSM, which are guaranteed to be semimetallic due to the specification of the symmetry content. These systems are exemplified by the 3D systems with inversion but not TR symmetries [13, 14].

Since reSMs are, by definition, also diagnosable using the representation content, one can systematically isolate them from $\{\text{BS}\}$. However, it is important to realize that reSMs do not form a subgroup of $\{\text{BS}\}$, since stacking two of them (say) may lead to a band insulator [13, 14]. In contrast, it is guaranteed that stacking two band insulators will lead to yet another band insulator. This suggests that we should identify the subgroup $\{\text{BI}\} \leq \{\text{BS}\}$. Further observe $\{\text{AI}\} \leq \{\text{BI}\}$, it is natural to define the following further diagnosis of the

elements in $\{\text{BS}\}$:

$$X_{\text{SM}} \equiv \frac{\{\text{BS}\}}{\{\text{BI}\}}; \quad X_{\text{BI}} \equiv \frac{\{\text{BI}\}}{\{\text{AI}\}}. \quad (\text{E1})$$

The nontrivial entries in X_{SM} and X_{BI} respectively correspond to reSMs and reQBIs. As we have alluded to, the nontrivial elements in X_{BS} are either reSMs or reQBIs, and hence, unsurprisingly, the three objects X_{BS} , X_{SM} and X_{BI} are not independent. From definitions, one can check that

$$X_{\text{SM}} = \frac{X_{\text{BS}}}{X_{\text{BI}}}. \quad (\text{E2})$$

Or in a more formal language, X_{BS} can be viewed as a central extension of X_{SM} by X_{BI} . Curiously, this extension is generally nontrivial. As a concrete example, consider the \mathbb{Z}_4 factor in $X_{\text{BS}} = \mathbb{Z}_2^3 \times \mathbb{Z}_4$ for SG **2** (inversion only) assuming no TR symmetry. From Refs. [13, 14], we see that the generator of this factor is a reSM (with inversion related Weyl points), and the ‘twice’ of that, corresponding to $2 \in \mathbb{Z}_4$, is a reQBI with a quantized magnetoelectric response of $\theta = \pi$. This shows that for this particular example,

$$X_{\text{BI}} = \mathbb{Z}_2^4; \quad X_{\text{SM}} = \mathbb{Z}_2, \quad (\text{E3})$$

and the \mathbb{Z}_4 factor in X_{BS} originates from the nontrivial extension of \mathbb{Z}_2 by \mathbb{Z}_2 .

2. reQBI

As we will discuss in the following, given any symmetry setting one can systematically study all reSMs using symmetry arguments together with knowledge on the generic stability of Fermi surfaces. For instance, for centrosymmetric systems with TR symmetry and significant SOC, stable band degeneracy must happen at a high-symmetry momentum, and therefore we can rule out the possibility of reSMs in these problems, i.e. for such settings we have $X_{\text{SM}} = \mathbb{Z}_1$ and hence $X_{\text{BI}} = X_{\text{BS}}$. However, even after X_{BI} is obtained our approach is still based on symmetry-labels in nature, and therefore does not necessarily detect all nontrivial phases. An important future direction is to incorporate the tenfold way classification into our current framework, akin to the arguments given in Ref. [22]. We further conjecture that once this is achieved, one will arrive at a complete classification of QBIs in the symmetry setting, and that this classification is equivalent to quotienting out all atomic insulators from the K-theory classification of Ref. [23].

3. reSM

For a TB model with the inversion symmetry but without the TR symmetry, some combinations of the parity eigenvalues at TRIMs predict the existence of Weyl points somewhere in the interior of the BZ [13, 14]. The semimetallic behavior of such systems is enforced by the specification of the irreps,

and we refer to such systems as ‘reSMs’. In this section, we ask whether similar phenomena occur for other SGs. Namely, given a SG and a set of integers \mathbf{n} for irreps at high-symmetry momenta, can we predict the existence of Weyl points somewhere at non-high-symmetry points in BZ?

To answer this question, let us consider a unit sphere S^2 around the Γ point of the BZ. The radius of the sphere is set to be much smaller than any reciprocal lattice vectors. If there are Weyl points at generic momenta in the BZ (i.e. not high-symmetry), we should be able to move them to the surface of this sphere without breaking any symmetry or changing the value of \mathbf{n} . Note that, in the following ‘sphere’ always refer to S^2 , which does not include the interior of the sphere.

An SG element $g \in \mathcal{G}$ moves a point \mathbf{k} on S^2 to $p_g \mathbf{k}$ on S^2 . For this transformation, the translation part \mathbf{t}_g of g does not show up at all and hence what is really important is the point group $\mathcal{P} \simeq \mathcal{G}/T$ of the SG, whose elements are the orthogonal matrices p_g ($g \in \mathcal{G}$). There are only 32 crystallographic point groups in 3D, and we will systematically discuss them in the following. One can introduce the notation of the little group, the symmetry orbit, and Wyckoff positions to this S^2 in the same way as before. Given \mathbf{k} on S^2 , the little group $\mathcal{G}_{\mathbf{k}}$ is defined as

$$\mathcal{G}_{\mathbf{k}} = \{p_g \in \mathcal{P} : p_g \mathbf{k} = \mathbf{k}\}. \quad (\text{E4})$$

The symmetry orbit of \mathbf{k} (aka the star of \mathbf{k}) is defined as $\{p_g \mathbf{k} : p_g \in \mathcal{P}\}$. Also, two points \mathbf{k}_1 and \mathbf{k}_2 belong to the same (momentum-space) Wyckoff position iff there exists $g \in \mathcal{G}$ such that $\mathcal{G}_{\mathbf{k}_2} = p_g \mathcal{G}_{\mathbf{k}_1} p_g^{-1}$. Finally, let us define the irreducible part (or the fundamental domain) F of the sphere. The fundamental domain F tessellates the S^2 under the action of \mathcal{P} . Namely, any point on the sphere can be uniquely represented as $p_g \mathbf{k}$, where $\mathbf{k} \in F$ and $p_g \in \mathcal{P}$.

With this preparation, let us discuss the stability of the Weyl points against symmetry preserving deformations. Suppose that the fundamental domain F contains a Weyl point with the chirality $+1$. (By assumption, generically this Weyl point does not sit at the boundary of F .) Then there must be at least $|\mathcal{P}|$ Weyl points on the sphere in total. The domain $p_g F$ will contain a Weyl point with the chirality $\det[p_g]$. Suppose first that $\det[p_g] = +1$ for all $p_g \in \mathcal{P}$. This is the case for 11 out of 32 point groups in 3D. In this case, since the net chirality in the entire BZ must vanish, there must be another Weyl point in F with the chirality -1 (that belongs to a separate symmetry orbit), and the two Weyl points with the opposite chirality will freely annihilate with each other. This implies reSMs cannot exist for SGs with these point groups.

Next we discuss the remaining $32 - 11 = 21$ point groups, which always have half of the elements having $\det[p_g] = -1$. Again the number of symmetry-related Weyl points is $|\mathcal{P}|$, but now $|\mathcal{P}|/2$ of them has $+1$ chirality and the other half has the -1 chirality. A priori, this could be compatible with a reSM, since the net Weyl charge in the entire BZ vanishes. However, this still requires further symmetry analysis. We ask if one can move Weyl points on S^2 and merge pairs of them with opposite chirality without breaking the SG symmetry or changing the number of irreps \mathbf{n} . We found that 18 of the 21 remaining point groups contain at least one mirror reflection

symmetry and there exists a Wyckoff position on the sphere which is symmetric only under the mirror. For these point groups, two Weyl points with the opposite chirality will annihilate at this Wyckoff position. This again rules out reSMs in these settings.

The remaining three point groups are $\bar{1}$, $\bar{3}$, and $\bar{4}$ in the Hermann-Mauguin notation. $\bar{1}$ is the point group generated by the inversion symmetry, and we know that Weyl points can be protected by \mathbf{n} in this case [13, 14]. $\bar{3}$ contains $\bar{1}$ as a subgroup. The only possibly new candidate is thus the point group $\bar{4}$, which is the point group of the SG symmetry $\mathbf{8I}$ and $\mathbf{82}$. We looked at $\mathbf{8I}$ for the spinful but TR breaking setting and found that all generators of X_{BS} are gapped. We will leave a more careful search for new reSMs, possible in a handful of remaining settings, for a future study.

Appendix F: Details of models

1. leSM

As a concrete example, we consider a TR-symmetric system in SG 219 with significant spin-orbit coupling. We will see that, although band insulators are generally possible at a filling of $\nu = 4$ electrons per unit cell [31, 32], for a particular lattice specification a semimetallic behavior is unavoidable at this filling. This arises from the fact that, given the available symmetry irreps specified by the lattice, there is no way to satisfy all the compatibility relations at the filling $\nu = 4$, a claim we can readily verify using the basis of {BS}.

We now discuss the details of the example and construct a tight-binding model realizing the proposed leSM. We consider a lattice in Wyckoff position ‘ a ’, which contains two sites at $\mathbf{r}_1 \equiv \{0, 0, 0\}$ and $\mathbf{r}_2 \equiv \{1/2, 0, 0\}$ in the unit cell. The two sites are related by a glide symmetry. We suppose the physically relevant degrees of freedom arise from the three $p_{x,y,z}$ orbitals on each site, which together with electron spin leads to a 6-dimensional local Hilbert space. We will let \mathbf{L} and \mathbf{S} respectively denote the orbital and spin angular momentum operators in the single-particle basis.

As described in the main text, we consider a TR-symmetric system with a strong crystal-field splitting:

$$H_{\Delta} = \Delta \sum_{\mathbf{r}: \text{all sites}} \mathbf{c}_{\mathbf{r}}^{\dagger} (\mathbf{L} \cdot \mathbf{S}) \mathbf{c}_{\mathbf{r}}, \quad (\text{F1})$$

where $\mathbf{c}_{\mathbf{r}}$ represent the 6-dimensional (row) vector corresponding to the internal degrees of freedom. One can verify that when $\Delta > 0$, H_{Δ} splits the local energy levels to a spin-1/2 doublet lying below the spin-3/2 multiplet. (Note that when TR symmetry is absent, the spin-3/2 multiplet can be further split into two two dimensional irreps.) As discussed, we assume Δ is the dominant energy scale in the problem, which implies the low-lying spin-1/2 states are fully filled, and can be decoupled from the description of the system. This leaves behind the half-filled spin-3/2 multiplet, which corresponds to an effective eight-band model at filling $\nu = 4$.

Next we consider a nearest-neighbor hopping term

$$H_{t,\lambda} = \sum_{g \in \mathcal{G}} g (\mathbf{c}_{\mathbf{r}_1}^{\dagger} (t + \lambda \hat{\mathbf{x}} \cdot (\mathbf{L} \times \mathbf{S})) \mathbf{c}_{\mathbf{r}_2}) g^{\dagger} + \text{h.c.}, \quad (\text{F2})$$

where h.c. denotes Hermitian conjugate, and the notation $\sum_{g \in \mathcal{G}} g (\dots) g^{\dagger}$ denotes all the terms generated by transforming the bond in the parenthesis by the symmetry elements of the SG \mathcal{G} .

The band structure of the full Hamiltonian $H = H_{\Delta} + H_{t,\lambda}$ is shown in Fig. 2c, with parameters $(t/\Delta, \lambda/\Delta) = (0.01, 0.05)$. As our computation dictates, the spin-3/2 multiplet gives rise to energy bands that are necessarily gapless along the high-symmetry lines at filling $\nu = 4$. Interestingly, note that the lattice-enforced gaplessness is of a more subtle flavor: Unlike spinless graphene, where the gaplessness is enforced by the dimensions of the irreps involved, here all the irreps have dimensions ≤ 4 , and therefore the impossibility of finding a BS at $\nu = 4$ is reflected in the connectivity of the energy bands.

In closing, we remark that the notion of ‘leSM’ is not as robust as the other notions we introduced in this work, say ‘feSM’ or ‘reQBI’. Specifically, the (semi-)metallic behavior of the system is protected by the assumed microscopic degrees of freedom, which is only sensible assuming a certain knowledge about the energetics of the problem. Under stacking of a trivial phase, say when we incorporate into the description a set of fully filled bands corresponding to an atomic insulator, the enforced gaplessness may become unstable as these apparently inert degrees of freedom can also supply the representations needed to open a gap at the targeted filling. This can be readily seen from the example above: If we switch the sign of Δ , the same electron filling will now correspond to the full filling of the spin-3/2 multiplet, which leads to an atomic insulator. Such instability should be contrasted with, say, the notion of reQBIs, which by definition remains nontrivial as long as the extra DOF we introduce are in the trivial class, i.e. correspond to AIs.

2. TR-breaking spinless feQBIs

A band insulator, invariant under a set of symmetries (including an SG \mathcal{G}), is called a feQBI if the number of the occupied bands (i.e., the filling) is different from that of any AIs with the same symmetry. By knowing the filling alone, we can thus tell that the insulator cannot be smoothly deformed into any AIs without breaking the symmetry. FeQBIs for TR-invariant spinful fermions are studied in details in Ref. [24]. Here we discuss feQBIs for spinless fermions.

FeQBIs for spinless fermions necessarily break the TR symmetry. This is because of the following reason: If there existed a TR-symmetric feQBI for spinless fermions, we could immediately construct a TR-symmetric feQBI for spinful fermions with the spin SU(2) symmetry. However, we know that the latter does not exist according to Ref. [24].

Furthermore, feQBIs for spinless fermions can possibly occur only in those 12 SGs listed in Table II. To see this, we should focus on (the maximal) fixed-point-free subgroups Γ

TABLE II. The set of fillings that correspond to at least one AI ($\mathcal{S}_{\mathcal{G}}^{\text{AI}}$) and BI ($\mathcal{S}_{\mathcal{G}}^{\text{BI}}$). $\mathcal{S}_{\mathcal{G}}^{\Gamma}$ is the set of BI fillings for fixed-point free subgroup Γ of \mathcal{G} . By definition, we have $\mathcal{S}_{\mathcal{G}}^{\text{AI}} \leq \mathcal{S}_{\mathcal{G}}^{\text{BI}} \leq \mathcal{S}_{\mathcal{G}}^{\Gamma}$, and in fact $\mathcal{S}_{\mathcal{G}}^{\text{AI}} = \mathcal{S}_{\mathcal{G}}^{\text{BI}} = \mathcal{S}_{\mathcal{G}}^{\Gamma}$ for all 218 SGs not listed here.

| \mathcal{G} | $\mathcal{S}_{\mathcal{G}}^{\text{AI}}$ | $\mathcal{S}_{\mathcal{G}}^{\text{BI}}$ | $\mathcal{S}_{\mathcal{G}}^{\Gamma}$ |
|-----------------------------|---|---|--------------------------------------|
| 106,110 | $4\mathbb{Z}_{\geq 0}$ | $2\mathbb{Z}_{\geq 0}$ | $2\mathbb{Z}_{\geq 0}$ |
| 73,133,142, 206, 228 | $4\mathbb{Z}_{\geq 0}$ | $2\mathbb{Z}_{\geq 0} \setminus \{2\}$ | $2\mathbb{Z}_{\geq 0}$ |
| 135 | $4\mathbb{Z}_{\geq 0}$ | $4\mathbb{Z}_{\geq 0}$ | $2\mathbb{Z}_{\geq 0}$ |
| 199, 214 | $2\mathbb{Z}_{\geq 0} \setminus \{2\}$ | $2\mathbb{Z}_{\geq 0} \setminus \{2\}$ | $2\mathbb{Z}_{\geq 0}$ |
| 220 | $2\mathbb{Z}_{\geq 0} \setminus \{2, 4, 10\}$ | $2\mathbb{Z}_{\geq 0} \setminus \{2\}$ | $2\mathbb{Z}_{\geq 0}$ |
| 230 | $4\mathbb{Z}_{\geq 0} \setminus \{4\}$ | $2\mathbb{Z}_{\geq 0} \setminus \{2, 4\}$ | $2\mathbb{Z}_{\geq 0}$ |

TABLE III. The summary of X_{BS} and its generators for the 12 SGs listed in Table II.

| \mathcal{G} | X_{BS} | Generator of X_{BS} |
|-----------------------------|-----------------|------------------------------|
| 106,110 | \mathbb{Z}_2 | feQBI at filling 2 |
| 73,133,142, 206, 228 | \mathbb{Z}_2 | feQBI at filling 6 |
| 135 | 1 | — |
| 199, 214 | 1 | — |
| 220 | \mathbb{Z}_2 | feQBI at filling 4 |
| 230 | \mathbb{Z}_2 | feQBI at filling 6, 10 |

of \mathcal{G} (not to be confused with the Γ point in BZ). For a fixed-point-free SG Γ , it is easy to show that a certain number of bands must cross with each other somewhere at high-symmetry points or on high-symmetry lines, and that the BI fillings are integer multiples of $\nu_{\Gamma} > 1$. Hence, if \mathcal{G} contains Γ as a subgroup, we know that any \mathcal{G} -symmetric BI should have a filling $\nu_{\Gamma}n$. For all 218 SGs not listed in Table II, there exists a \mathcal{G} -symmetric AI with the filling ν_{Γ} . Hence, there cannot be any mismatch of the filling between BI and AI for them. On the other hand, for 9 SGs out of the 12 SGs in Table II, we found that X_{BS} is nontrivial and it is generated by feQBI as summarized in Table III.

Before moving on to a specific example, let us remark on the Table II. In this table, we show the set of fillings $\mathcal{S}_{\mathcal{G}}^{\text{AI}}$ that correspond to at least one AI. This set was computed by the following way. Let $\nu_{\mathbf{x},r}$ be the filling of the AI arising from fully occupying a site-symmetry group irrep $u_{\mathbf{x}}^r$ of the position \mathbf{x} . Then we take superpositions with non-negative integer coefficients: $\mathcal{S}_{\mathcal{G}}^{\text{AI}} = \{\sum_{\mathbf{x},r} m_{\mathbf{x},r} \nu_{\mathbf{x},r} : m_{\mathbf{x},r} \in \mathbb{Z}_{\geq 0}\}$, which is, in principle, different from the fillings for $\{\text{AI}\} \cap \mathbb{Z}_{\geq 0}^D$. On the other hand, $\mathcal{S}_{\mathcal{G}}^{\text{BI}}$ is simply the fillings for $\{\text{BI}\} \cap \mathbb{Z}_{\geq 0}^D$.

As a concrete example of TR breaking spinless feQBI, let us discuss **106**, which hosts feQBI at filling 2. Consider a tight-binding model (4 band model) defined on \mathcal{W}_b^{106} with one orbital per site. Here, \mathcal{W}_b^{106} means the Wyckoff position with the Wyckoff letter b in Ref. [28]:

$$\left(0, \frac{1}{2}, z\right), \left(\frac{1}{2}, 0, z + \frac{1}{2}\right), \left(\frac{1}{2}, 0, z\right), \left(0, \frac{1}{2}, z + \frac{1}{2}\right) \quad (\text{F3})$$

TABLE IV. The symmetry setting for feQBIs in Table III. With a proper choice of $h_{\mathbf{k}}$, one can realize a band gap between the ν -th and $\nu + 1$ -th bands. m_{tot} is the total number of bands in this setting. The s orbital is the trivial representation (i.e., $u(g) = 1$ for all $g \in \mathcal{G}_{\mathbf{x}}$). The site symmetry group for the Wyckoff position b of **106** and the Wyckoff position a of **110** are an order 2 group, and the p orbital refers to the representation with -1 for the non-identity element. The site symmetry group for the Wyckoff position a of **230** is $\bar{3}$ group, generated by the improper three-fold rotation IC_3 . The p orbital refers to the one that has $e^{i\frac{2\pi}{6}}$ eigenvalue of IC_3 .

| \mathcal{G} | Wyckoff position | w orbital | m_{tot} | ν |
|-------------------------|------------------|-------------|------------------|-------|
| 106 | b | p | 4 | 2 |
| 110 | a | p | 4 | 2 |
| 133 | $a + e$ | s | 12 | 6 |
| 220 | c | s | 8 | 4 |
| 228(>142, 73) | d | s | 12 | 6 |
| 230(>206) | a | $s + p$ | 16 | 6,10 |

The site symmetry of this Wyckoff position is the π -rotation about the z -axis. We use the ‘ p orbital’ that flips sign under the rotation. These informations specify the representation $[U_{\mathbf{k}}(g)]_{\sigma'j,\sigma i} \equiv [U_{\mathbf{x}}^a(g)]_{\sigma'jk',\sigma ik}$ of $\mathcal{G} = \mathbf{106}$ in the TB model. (In this particular example, i, j label can be dropped since the orbital is a 1D representation). In this notation, $U_{\mathbf{k}}(g)$ satisfies multiplication rule $U_{p_{g_2}\mathbf{k}}(g_1)U_{\mathbf{k}}(g_2) = U_{\mathbf{k}}(g_1g_2)$.

We construct a \mathcal{G} -symmetric Hamiltonian $H_{\mathbf{k}}$ in two steps: (i) we choose an arbitrary 4 by 4 Hermitian matrix $h_{\mathbf{k}}$ and (ii) symmetrize $h_{\mathbf{k}}$ by performing summation:

$$H_{\mathbf{k}} = \sum_{g \in \mathcal{G}/T} U_{\mathbf{k}}(g)^{\dagger} h_{p_g\mathbf{k}} U_{\mathbf{k}}(g). \quad (\text{F4})$$

After the summation, $H_{\mathbf{k}}$ automatically fulfills the symmetry requirement, i.e., $H_{p_g\mathbf{k}} U_{\mathbf{k}}(g) = U_{\mathbf{k}}(g) H_{\mathbf{k}}$.

To realize an example of feQBI for **106**, the following choice of $h_{\mathbf{k}}$ works

$$h_{\mathbf{k}} = \Delta \begin{pmatrix} (\cos k_x - \cos k_y) & 1 & 0 & -i \\ & 1 & 0 & 0 \\ & 0 & 0 & -i \\ & i & 0 & i \end{pmatrix}, \quad (\text{F5})$$

where Δ sets the energy scale of the problem. The symmetrized Hamiltonian $H_{\mathbf{k}}$ has a very large gap. At each \mathbf{k} , let $\delta E_{\mathbf{k}}$ be the band gap between the second and the third band and $W_{\mathbf{k}}$ be the band width (the energy difference between the lowest and the highest band). Then we found $\delta E = 0.33W$ where $\delta E = \min_{\mathbf{k}} \delta E_{\mathbf{k}}$ and $W = \max_{\mathbf{k}} W_{\mathbf{k}}$. We also found that the Chern numbers of the TB model is zero.

In Table IV, we list an example of symmetry settings for feQBIs in other SGs.

3. TR-symmetric feQBIs

Finally, we briefly comment on the implications of the present work on the feQBIs we introduced in Ref. [24], which arise in systems with TR symmetry and significant SOC. There, the focus of study are SGs **199**, **214**, **220** and **230**, which have an intriguing property in the ratios between the Wyckoff position multiplicities: They were dubbed ‘Wyckoff-mismatched’ as some Wyckoff multiplicities are not integer multiples of the smallest one. In these systems, it was realized that QBIs are possible at non-atomic fillings, and hence the name feQBIs.

However, in the analysis of Ref. [24] the mismatch between BSs and AIs is discussed in terms of their corresponding physical fillings, which as we have explained is a stronger condition than that exposed using only the abelian group structures of $\{\text{BS}\}$ and $\{\text{AI}\}$. As a result, these feQBIs could be trivial in X_{BS} . This is indeed the case for some of them: both **199** and **214** have no nontrivial BSs in $X_{\text{BS}} = \mathbb{Z}_1$. (By our convention, they are omitted from Table I.)

It remains to study **220** and **230**, which have $X_{\text{BS}} = \mathbb{Z}_2$ and \mathbb{Z}_4 respectively. We found that for both cases, some feQBIs are again in the trivial class, i.e. they can be understood as integer combinations of AIs (but with negative coefficients,

resulting in unrealizable AI upon enforcing the physical conditions). However, the nontrivial class for **220** can be represented by a feQBI filling $\nu = 20$. More interestingly, the entry $2 \in \mathbb{Z}_4$ for **230** can be represented by a feQBI at filling $\nu = 8$. Since **230** is centrosymmetric, as we have argued in the main text the generator $1 \in \mathbb{Z}_4$ has to be identified with the strong TI. This implies some $\nu = 8$ feQBIs in **230** realize the ‘doubled strong TI’ phase we discussed in the main text, which has inversion-protected nontrivial entanglement signature, albeit no physical surface state is expected.

All in all, we found that generally the TR-symmetric feQBIs do not have any simple relationship with X_{BS} , although there are indeed examples which are nontrivial from both perspectives.

Appendix G: Tables of X_{BS} and $d_{\text{BS}} = d_{\text{AI}}$

The obtained classifications X_{BS} in the other three symmetry settings (with/ without SOC or TR) are tabulated in Tables V - VII. In Tables VIII - XI we provide tables for the computed values of $d \equiv d_{\text{BS}} = d_{\text{AI}}$. We adopt the same color code as in Table I in the main text.

TABLE V. Spinful without TR

| X_{BS} | SGs |
|--|---|
| \mathbb{Z}_2 | <i>3, 11, 14, 48, 49, 50, 52, 53, 54, 56, 57, 58, 59, 60, 61, 62, 63, 64, 66, 67, 68, 70, 72, 73, 74</i> <i>77, 79, 111, 112, 113, 114, 115, 116, 117, 118, 119, 120, 121, 122, 125, 126, 129, 130, 133, 134, 137, 138, 141, 142, 162</i> <i>163, 164, 165, 166, 167, 171, 172, 201, 203, 205, 206, 215, 216, 217, 218, 219, 220, 222, 224, 227, 228, 230</i> |
| \mathbb{Z}_3 | <i>143, 173, 188, 190</i> |
| \mathbb{Z}_4 | <i>69, 71, 75, 124, 128, 132, 135, 136, 140, 202, 204, 223, 226</i> |
| \mathbb{Z}_6 | <i>168, 192, 193, 194</i> |
| \mathbb{Z}_8 | <i>139, 225, 229</i> |
| $\mathbb{Z}_2 \times \mathbb{Z}_2$ | <i>12, 13, 15, 51, 55, 86, 88</i> |
| $\mathbb{Z}_2 \times \mathbb{Z}_4$ | <i>65, 84, 85, 131, 148, 200</i> |
| $\mathbb{Z}_2 \times \mathbb{Z}_{12}$ | <i>147</i> |
| $\mathbb{Z}_3 \times \mathbb{Z}_3$ | <i>187, 189</i> |
| $\mathbb{Z}_3 \times \mathbb{Z}_6$ | <i>176</i> |
| $\mathbb{Z}_4 \times \mathbb{Z}_4$ | <i>87, 127</i> |
| $\mathbb{Z}_4 \times \mathbb{Z}_8$ | <i>221</i> |
| $\mathbb{Z}_6 \times \mathbb{Z}_{12}$ | <i>191</i> |
| $\mathbb{Z}_2 \times \mathbb{Z}_2 \times \mathbb{Z}_2$ | <i>10, 82</i> |
| $\mathbb{Z}_2 \times \mathbb{Z}_2 \times \mathbb{Z}_4$ | <i>81</i> |
| $\mathbb{Z}_2 \times \mathbb{Z}_4 \times \mathbb{Z}_8$ | <i>123</i> |
| $\mathbb{Z}_3 \times \mathbb{Z}_3 \times \mathbb{Z}_3$ | <i>174</i> |
| $\mathbb{Z}_4 \times \mathbb{Z}_4 \times \mathbb{Z}_4$ | <i>83</i> |
| $\mathbb{Z}_6 \times \mathbb{Z}_6 \times \mathbb{Z}_6$ | <i>175</i> |
| $\mathbb{Z}_2 \times \mathbb{Z}_2 \times \mathbb{Z}_2 \times \mathbb{Z}_4$ | <i>2, 47</i> |

TABLE VI. Spinless with TR

| X_{BS} | SGs |
|--|--|
| \mathbb{Z}_2 | <i>3, 11, 14, 27, 37, 48, 49, 50, 52, 53, 54, 56, 58, 60, 66, 68, 70, 75, 77, 82, 85, 86, 88, 103, 124, 128, 130, 162, 163, 164, 165, 166, 167, 168, 171, 172, 176, 184, 192, 201, 203</i> |
| $\mathbb{Z}_2 \times \mathbb{Z}_2$ | <i>12, 13, 15, 81, 84, 87</i> |
| $\mathbb{Z}_2 \times \mathbb{Z}_4$ | <i>147, 148</i> |
| $\mathbb{Z}_2 \times \mathbb{Z}_2 \times \mathbb{Z}_2$ | <i>10, 83, 175</i> |
| $\mathbb{Z}_2 \times \mathbb{Z}_2 \times \mathbb{Z}_2 \times \mathbb{Z}_4$ | <i>2</i> |

TABLE VII. Spinless without TR

| X_{BS} | SGs |
|--|--|
| \mathbb{Z}_2 | <i>3, 11, 14, 27, 37, 45, 48, 49, 50, 52, 53, 54, 56, 58, 60, 61, 66, 68, 70, 73, 77, 79, 103, 104, 106, 110, 112, 114, 116, 117, 118, 120, 122, 126, 130, 133, 142, 162, 163, 164, 165, 166, 167, 171, 172, 184, 201, 203, 205, 206, 218, 219, 220, 222, 228, 230</i> |
| \mathbb{Z}_3 | <i>143, 173, 188, 190</i> |
| \mathbb{Z}_4 | <i>75, 124, 128</i> |
| \mathbb{Z}_6 | <i>168, 192</i> |
| $\mathbb{Z}_2 \times \mathbb{Z}_2$ | <i>12, 13, 15, 86, 88</i> |
| $\mathbb{Z}_2 \times \mathbb{Z}_4$ | <i>84, 85, 148</i> |
| $\mathbb{Z}_2 \times \mathbb{Z}_{12}$ | <i>147</i> |
| $\mathbb{Z}_3 \times \mathbb{Z}_6$ | <i>176</i> |
| $\mathbb{Z}_4 \times \mathbb{Z}_4$ | <i>87</i> |
| $\mathbb{Z}_2 \times \mathbb{Z}_2 \times \mathbb{Z}_2$ | <i>10, 82</i> |
| $\mathbb{Z}_2 \times \mathbb{Z}_2 \times \mathbb{Z}_4$ | <i>81</i> |
| $\mathbb{Z}_3 \times \mathbb{Z}_3 \times \mathbb{Z}_3$ | <i>174</i> |
| $\mathbb{Z}_4 \times \mathbb{Z}_4 \times \mathbb{Z}_4$ | <i>83</i> |
| $\mathbb{Z}_6 \times \mathbb{Z}_6 \times \mathbb{Z}_6$ | <i>175</i> |
| $\mathbb{Z}_2 \times \mathbb{Z}_2 \times \mathbb{Z}_2 \times \mathbb{Z}_4$ | <i>2</i> |

TABLE VIII. Spinful with TR

| d | SGs |
|-----|---|
| 1 | <i>1, 3, 4, 5, 6, 7, 8, 9, 16, 17, 18, 19, 20, 21, 22, 23, 24, 25, 26, 27, 28, 29, 30, 31, 32, 33, 34, 35, 36, 37</i> <i>38, 39, 40, 41, 42, 43, 44, 45, 46, 76, 77, 78, 80, 91, 92, 93, 94, 95, 96, 98, 101, 102, 105, 106, 109, 110, 144, 145, 151, 152</i> <i>153, 154, 169, 170, 171, 172, 178, 179, 180, 181</i> |
| 2 | <i>79, 90, 97, 100, 104, 107, 108, 146, 155, 160, 161, 195, 196, 197, 198, 199, 208, 210, 212, 213, 214</i> |
| 3 | <i>48, 50, 52, 54, 56, 57, 59, 60, 61, 62, 68, 70, 73, 75, 89, 99, 103, 112, 113, 114, 116, 117, 118, 120, 122, 133, 142, 150, 157, 159</i> <i>173, 182, 185, 186, 209, 211</i> |
| 4 | <i>63, 64, 72, 121, 126, 130, 135, 137, 138, 143, 149, 156, 158, 168, 177, 183, 184, 207, 218, 219, 220</i> |
| 5 | <i>11, 13, 14, 15, 49, 51, 53, 55, 58, 66, 67, 74, 81, 82, 86, 88, 111, 115, 119, 134, 136, 141, 167, 217, 228, 230</i> |
| 6 | <i>69, 71, 85, 125, 129, 132, 163, 165, 190, 201, 203, 205, 206, 215, 216, 222</i> |
| 7 | <i>12, 65, 84, 128, 131, 140, 188, 189, 202, 204, 223</i> |
| 8 | <i>124, 127, 148, 166, 193, 200, 224, 226, 227</i> |
| 9 | <i>2, 10, 47, 87, 139, 147, 162, 164, 176, 192, 194</i> |
| 10 | <i>174, 187</i> |
| 11 | <i>225, 229</i> |
| 13 | <i>83, 123</i> |
| 14 | <i>175, 191, 221</i> |

TABLE IX. Spinful without TR

| d | SGs |
|-----|--|
| 1 | <i>1, 4, 7, 9, 16, 19, 22, 23, 25, 26, 27, 29, 33, 36, 38, 39, 42, 44, 45, 76, 78, 93, 101, 105, 109, 110, 144, 145, 169, 170</i> <i>180, 181</i> |
| 2 | <i>8, 21, 31, 35, 37, 41, 43, 46, 80, 92, 94, 96, 97, 98, 102, 106, 107, 108, 161, 208, 214</i> |
| 3 | <i>5, 6, 18, 20, 30, 32, 34, 40, 48, 50, 56, 59, 61, 62, 68, 70, 73, 89, 99, 103, 146, 151, 152, 153, 154, 160, 171, 172, 178, 179</i> <i>185, 186, 195, 196, 197, 198, 209, 210, 211, 212, 213</i> |
| 4 | <i>24, 28, 54, 57, 60, 72, 77, 90, 91, 95, 100, 104, 133, 137, 142, 155, 158, 159, 177, 183, 184, 199, 207</i> |
| 5 | <i>3, 14, 17, 52, 63, 64, 67, 79, 111, 112, 115, 116, 119, 120, 121, 126, 130, 134, 138, 156, 157, 173, 182</i> |
| 6 | <i>11, 15, 49, 69, 71, 113, 114, 117, 118, 125, 129, 132, 135, 141, 149, 150, 215, 216, 217, 218, 219</i> |
| 7 | <i>13, 51, 55, 66, 74, 122, 131, 136, 143, 167, 220, 228, 230</i> |
| 8 | <i>58, 65, 75, 88, 140, 163, 165, 222, 223, 224</i> |
| 9 | <i>2, 47, 53, 86, 139, 168, 201, 203, 205, 206, 227</i> |
| 10 | <i>12, 187, 189, 193, 194, 202, 204, 226</i> |
| 11 | <i>82, 85, 124, 148, 166, 200, 225, 229</i> |
| 12 | <i>81, 127, 128, 162, 164, 188, 190</i> |
| 13 | <i>84, 123, 147, 192</i> |
| 14 | <i>191, 221</i> |
| 15 | <i>10</i> |
| 16 | <i>87, 176</i> |
| 21 | <i>174</i> |
| 24 | <i>83</i> |
| 27 | <i>175</i> |

TABLE X. Spinless with TR

| d | SGs |
|-----|---|
| 1 | <i>1, 4, 7, 9, 19, 29, 33, 76, 78, 144, 145, 169, 170</i> |
| 2 | <i>8, 31, 36, 41, 43, 80, 92, 96, 110, 146, 161, 198</i> |
| 3 | <i>5, 6, 18, 20, 26, 30, 32, 34, 40, 45, 46, 61, 106, 109, 151, 152, 153, 154, 159, 160, 171, 172, 173, 178, 179, 199, 212, 213</i> |
| 4 | <i>24, 28, 37, 39, 60, 62, 77, 79, 91, 95, 102, 104, 143, 155, 157, 158, 185, 186, 196, 197, 210</i> |
| 5 | <i>3, 14, 17, 27, 42, 44, 52, 56, 57, 94, 98, 100, 101, 108, 114, 122, 150, 156, 182, 214, 220</i> |
| 6 | <i>11, 15, 35, 38, 54, 70, 73, 75, 88, 90, 103, 105, 107, 113, 142, 149, 167, 168, 184, 195, 205, 219</i> |
| 7 | <i>13, 22, 23, 59, 64, 68, 82, 86, 117, 118, 120, 130, 163, 165, 180, 181, 203, 206, 208, 209, 211, 218, 228, 230</i> |
| 8 | <i>21, 58, 63, 81, 85, 97, 116, 133, 135, 137, 148, 183, 190, 201, 217</i> |
| 9 | <i>2, 25, 48, 50, 53, 55, 72, 99, 121, 126, 138, 141, 147, 188, 207, 216, 222</i> |
| 10 | <i>12, 74, 93, 112, 119, 176, 177, 202, 204, 215</i> |
| 11 | <i>66, 84, 128, 136, 166, 227</i> |
| 12 | <i>51, 87, 89, 115, 129, 134, 162, 164, 174, 189, 193, 223, 226</i> |
| 13 | <i>16, 67, 111, 125, 194, 224</i> |
| 14 | <i>49, 140, 192, 200</i> |
| 15 | <i>10, 69, 71, 124, 127, 132, 187</i> |
| 17 | <i>225, 229</i> |
| 18 | <i>65, 83, 131, 139, 175</i> |
| 22 | <i>221</i> |
| 24 | <i>191</i> |
| 27 | <i>47, 123</i> |

TABLE XI. Spinless without TR

| d | SGs |
|-----|--|
| 1 | <i>1, 4, 7, 9, 19, 29, 33, 76, 78, 144, 145, 169, 170</i> |
| 2 | <i>8, 31, 36, 41, 43, 80, 92, 96, 110, 161</i> |
| 3 | <i>5, 6, 18, 20, 26, 30, 32, 34, 40, 45, 46, 61, 106, 109, 146, 151, 152, 153, 154, 160, 171, 172, 178, 179, 198, 212, 213</i> |
| 4 | <i>24, 28, 37, 39, 60, 62, 77, 91, 95, 102, 155, 158, 159, 185, 186, 199, 210</i> |
| 5 | <i>3, 14, 17, 27, 42, 44, 52, 56, 57, 79, 94, 98, 101, 104, 108, 156, 157, 173, 182, 196, 197, 214</i> |
| 6 | <i>11, 15, 35, 38, 54, 70, 73, 100, 103, 105, 107, 149, 150, 184</i> |
| 7 | <i>13, 22, 23, 59, 64, 68, 90, 114, 122, 142, 143, 167, 180, 181, 195, 208, 209, 211, 220</i> |
| 8 | <i>21, 58, 63, 75, 88, 97, 113, 130, 137, 163, 165, 183, 219</i> |
| 9 | <i>2, 25, 48, 50, 53, 55, 72, 86, 99, 117, 118, 120, 133, 135, 141, 168, 205, 207, 216, 217, 218, 228, 230</i> |
| 10 | <i>12, 74, 93, 116, 119, 121, 126, 138, 177, 203, 206, 215</i> |
| 11 | <i>66, 82, 85, 148, 166, 201, 222, 227</i> |
| 12 | <i>51, 81, 89, 112, 115, 129, 134, 136, 162, 164, 188, 190</i> |
| 13 | <i>16, 67, 84, 111, 125, 147, 193, 194, 202, 204, 223, 224</i> |
| 14 | <i>49, 128, 226</i> |
| 15 | <i>10, 69, 71, 132, 140, 187, 189</i> |
| 16 | <i>87, 176</i> |
| 17 | <i>124, 192, 200, 225, 229</i> |
| 18 | <i>65, 127, 131, 139</i> |
| 21 | <i>174</i> |
| 22 | <i>221</i> |
| 24 | <i>83, 191</i> |
| 27 | <i>47, 123, 175</i> |